[IC_{50}(**3E**) = 0.234 μM (NL4-3) and 0.295 μM (IIIB); IC_{50}(**3F**) = 0.332 μM (NL4-3) and 0.403 μM (IIIB)]. The potency was significantly less compared with the original FC131 **2** [IC_{50}(**2**) = 0.014 μM (NL4-3) and 0.019 μM (IIIB)]. Substitutions of Arg3-Nal4 dipeptides with EADI and FADI resulted in the loss of the anti-HIV activity [IC_{50}(**4E**/**4F**) > 10 μM (NL4-3 and IIIB)], which also correlates with the observation of no CXCR4 antagonistic activity of these peptides. For the Ba-L strain, that utilizes CCR5 for entry, all peptides showed no inhibitory activity at 10 μM.

Conclusions

In conclusion, Orn-Orn type EADI **14** and Orn-Nal type FADI **18** were synthesized and incorporated into FC131 analogues. Comparative bioevaluation of a set of peptides containing EADI or FADI at Arg2-Arg3 and Arg3-Nal4 positions revealed the significant contribution of these peptide bonds to FC131 bioactivity. Although substitutions with alkene isosteres resulted in a decrease in bioactivity, the structural and functional requirements of the corresponding amide bonds to biological activity was shown. The results will be useful for the development of cyclic pentapeptide-based CXCR4 antagonists. Additionally, it was demonstrated that FC131 and the analogous were selective CXCR4 antagonists, which did not inhibit SDF-1 binding to CXCR7. Further studies on the synthesis and biological evaluation of CXCR4 antagonists with peptide bond mimetics are the subject of an ongoing investigation.

Experimental

Synthesis

***tert*-Butyl (2*R*,5*S*,3*E*)-8-[*N*-(benzyloxycarbonyl)amino]-2-[3-(*tert*-butyldimethylsiloxy)prop-1-yl]-5-[*N*-(*o*-nitrobenzenesulfonyl)amino]oct-3-enoate (10).** 1.57 M *t*-BuLi in *n*-pentane solution (28.7 cm^3, 45 mmol) was added dropwise to a stirred solution of $I(CH_2)_3OTBS$ (6.78 g, 22.5 mmol) in dry Et_2O (10.6 cm^3) under argon at −78 °C. Following stirring at −78 °C for 30 min, the mixture was stirred at room temperature for 10 min. To a stirred solution of CuCN (1.26 g, 14.1 mmol) and LiCl (1.19 g, 28.1 mmol) in dry THF (20 cm^3) under argon at −78 °C, the above 0.5 M $TBSO(CH_2)_3Li$ in THF–Et_2O–*n*-pentane solution (28.2 cm^3) was added dropwise, and the mixture was further stirred at 0 °C for 10 min. To the above mixture, a solution of the enoate **9** (1.92 g, 3.51 mmol) in dry THF (20 cm^3) was added dropwise at −78 °C, and the mixture was further stirred for 2 h at −78 °C. The reaction was quenched by the addition of a saturated NH_4Cl/28% NH_4OH solution (1/1, 30 cm^3), with additional stirring at room temperature for 1 h. After the mixture was concentrated under reduced pressure, the residue was extracted with Et_2O. The extract was washed with water and brine, and dried over $MgSO_4$. Concentration under reduced pressure followed by flash chromatography over silica gel with EtOAc–*n*-hexane (1/5) gave the title compound **10** (1.68 g, 66%) as a colorless oil: $[\alpha]_D^{24}$ −89.8 (*c* 1.00, $CHCl_3$); δ_H (500 MHz, $CDCl_3$, Me_4Si) 0.00 (6 H, s), 0.85 (9 H, s), 1.22–1.26 (2 H, m), 1.34 (9 H, s), 1.46–1.51 (6 H, m), 2.59–2.64 (1 H, m), 3.12–3.14 (2 H, m), 3.45–3.48 (2 H, m), 3.89–3.93 (1 H, m), 4.79–4.87 (1 H, m), 5.04 (2 H, s), 5.22 (1 H, dd, *J* 15.5 and 7.4), 5.34 (1H, dd, *J* 15.5 and 8.6), 5.42 (1 H, d, *J* 8.0), 7.23–7.31 (5 H, m), 7.61–7.65 (2 H, m), 7.74–7.80 (1 H, m) and 7.99–8.06 (1 H, m); δ_C (125 MHz, $CDCl_3$, Me_4Si) −5.4 (2 C), 18.2, 25.9 (3 C), 26.0, 27.9 (3 C), 28.7, 29.9, 33.0, 40.3, 49.0, 56.5, 62.5, 66.5, 80.6, 125.2, 128.0 (3 C), 128.4 (2 C), 130.9, 131.2, 132.8, 133.2, 133.3, 134.8, 136.5, 147.7, 156.4 and 172.6; HRMS (FAB), *m/z* calcd for $C_{35}H_{52}N_3O_9SSi$ ($[M - H]^-$) 718.3199, found 718.3190.

(2*R*,5*S*,3*E*)-8-[*N*-(Benzyloxycarbonyl)amino]-2-{3-[*N*-(benzyloxycarbonyl) amino]prop-1-yl}-5-[*N*-(fluorenylmethoxycarbonyl)amino]oct-3-enoic acid (14). Compound **13** (610 mg, 0.790 mmol) was dissolved in 4 N HCl–dioxane (8 cm^3) and the mixture was stirred at room temperature for 8 h. After the mixture was concentrated under reduced pressure, the residue was extracted with EtOAc. The extract was washed with 1 N HCl and brine, and dried over $MgSO_4$. Concentration under reduced pressure followed by flash chromatography over silica gel with EtOAc–*n*-hexane–AcOH (1/1/0.02) gave the title compound **14** (367 mg, 65%) as a white solid: mp 162–163 °C; $[\alpha]_D^{24}$ −16.6 (*c* 1.02, DMSO); δ_H (500 MHz, DMSO, Me_4Si) 1.38–1.40 (7 H, m), 1.55–1.66 (1 H, m), 2.87 (1 H, m), 2.97 (4 H, m), 3.93 (1 H, m), 4.17–4.24 (1 H, m), 4.24–4.31 (1 H, m), 4.96–5.03 (5 H, m), 5.47 (2 H, m), 7.28–7.41 (17 H, m), 7.65–7.69 (2 H, m), 7.86–7.88 (2 H, m) and 12.20 (1 H, s); δ_C (125 MHz, DMSO, Me_4Si) 26.1, 27.0, 29.2, 30.9, 40.0 (2 C), 46.7, 47.8, 51.9, 65.1, 65.2 (2 C), 120.0 (2 C), 125.2 (2 C), 127.0 (2 C), 127.5 (2 C), 127.6 (3 C), 127.7 (3 C), 128.3 (4 C), 133.2, 137.2 (2 C), 140.7, 143.8 (2 C), 143.9 (2 C), 156.1 (3 C) and 174.8; HRMS (FAB), *m/z* calcd for $C_{42}H_{44}N_3O_8$ ($[M - H]^-$) 718.3134, found 718.3125.

(2*R*,5*S*,3*Z*)-5-[(*tert*-Butoxycarbonyl)amino]-8-(*tert*-butyldimethylsiloxy)-4-fluoro-2-(naphthalen-2-ylmethyl)oct-3-enoyl (*S*)-sultam (16). To a suspension of CuI (2.22 g, 11.6 mmol) in THF (250 cm^3) at −78 °C under argon was added dropwise a solution of MeLi·LiBr complex in Et_2O (1.5 M, 15.5 cm^3, 23.2 mmol), and the mixture was stirred for 10 min at 0 °C. To the solution of the above organocopper reagent at −78 °C was added dropwise a solution of the *N*-enoyl sultam **15** (1.80 g, 2.90 mmol) in THF (70 cm^3). The mixture was stirred for 30 min at −78 °C and HMPA (8.31 cm^3, 46.4 mmol) was added dropwise to the mixture. After stirring for 30 min at −78 °C, a solution of triphenyltin chloride (2.24 g, 5.80 mmol) in THF (20 cm^3) was added dropwise, and the mixture was subsequently stirred for 10 min at −40 °C. 2-(Bromomethyl)naphthalene (5.13 g, 23.2 mmol) in THF (30 cm^3) was added dropwise and the mixture was stirred for 20 h at −40 °C. The reaction was quenched at −40 °C by the addition of a saturated NH_4Cl/28% NH_4OH solution (1/1, 50 cm^3) and the mixture was stirred at room temperature for an additional 30 min. The mixture was extracted with Et_2O and the extract was washed with brine and dried over $MgSO_4$. Concentration under reduced pressure followed by flash chromatography over silica gel with EtOAc–*n*-hexane (1/3) gave the title compound **16** (1.71 g, 79%) as a colorless oil: $[\alpha]_D^{24}$ −74.3 (*c* 1.00, $CHCl_3$); δ_H (500 MHz, $CDCl_3$, Me_4Si) 0.02 (6 H, s), 0.30 (3 H, s), 0.76 (3 H, s), 0.88 (9 H, s), 1.18–1.30 (2 H, m), 1.38–1.48 (11 H, m), 1.52–1.66 (4 H, m), 1.70–1.82 (2 H, m), 1.91 (1 H, dd, *J* 13.7 and 8.0), 2.97 (1 H, dd, *J* 13.7 and 6.9), 3.24–3.36 (3 H, m), 3.46–3.56 (2 H, m), 3.64–3.79 (1 H, m), 4.08–4.21 (1 H, m), 4.48–4.60 (1 H, m), 4.67 (1 H, d, *J* 8.6), 5.06 (1 H, dd, *J* 36.1 and 9.2), 7.38–7.44 (3 H, m), 7.64 (1 H, s) and 7.71–7.78 (3 H, m); δ_C (125 MHz, $CDCl_3$, Me_4Si) −5.3

(2 C), 18.3, 19.6, 19.8, 26.0 (3 C), 26.3, 28.3 (3 C), 28.6, 28.7, 32.8, 38.2, 40.6 (d, *J* 2.4), 43.0, 44.5, 47.3, 48.0, 51.7, 52.9, 62.5, 64.9, 79.6, 103.7 (d, *J* 13.1), 125.3, 125.7, 127.5, 127.6, 127.8, 127.9, 127.9, 132.4, 133.4, 135.1, 154.9, 158.8 (d, *J* 261.1) and 172.2; δ_F (125 MHz, $CDCl_3$, $CFCl_3$) −119.5; HRMS (FAB), *m/z* calcd for $C_{40}H_{58}FN_2O_6SSi$ ([M − H]$^-$) 741.3774, found: 741.3768.

(2*R*,5*S*,3*Z*)-5-[*N*-(Fluorenylmethoxycarbonyl)amino]-4-fluoro-2-(naphthalen-2-ylmethyl)-8-[*N*-(*o*-nitrobenzenesulfonyl)amino]oct-3-enoic acid (18). To a solution of the sultam **17** (986 mg, 1.08 mmol) and aqueous 50% H_2O_2 (0.383 cm^3, 5.62 mmol) in THF–H_2O (5/1, 15 cm^3) at 0 °C was added aqueous 1 N LiOH (2.16 cm^3, 2.16 mmol). The mixture was stirred at room temperature for 2 h. Following dilution with EtOAc (50 cm^3), the mixture was washed with 0.1 N HCl and dried over $MgSO_4$. Concentration under reduced pressure gave the corresponding acid, which was used in the next step without purification. TFA (5 cm^3) was added to a solution of the acid in CH_2Cl_2 (5 cm^3) at 0 °C, and the mixture was stirred at room temperature for 30 min. Concentration under reduced pressure gave an oily residue, which was dissolved in MeCN–DMF–H_2O (10/9/1, 40 cm^3). Fmoc-OSu (584 mg, 1.73 mmol) and Et_3N (0.332 cm^3, 2.38 mmol) were added to the mixture at 0 °C and the mixture was stirred at room temperature for 12 h. After being diluted with EtOAc (280 cm^3), the reaction mixture was washed with 1 N HCl and dried over $MgSO_4$. Concentration under reduced pressure followed by flash chromatography over silica gel with EtOAc–*n*-hexane–AcOH (1/1/0.02) gave the title compound **18** (673 mg, 85%) as a colorless semisolid: $[\alpha]_D^{25}$ −27.4 (*c* 1.00, $CHCl_3$); δ_H (500 MHz, $CDCl_3$, Me_4Si) 1.31–1.40 (2 H, m), 1.41–1.55 (2 H, m), 2.93–2.99 (3 H, m), 3.28 (1 H, dd, *J* 13.7 and 6.3), 3.78–3.87 (1 H, m), 4.08–4.16 (2 H, m), 4.28 (1 H, dd, *J* 10.3 and 6.9), 4.40 (1 H, dd, *J* 10.3 and 6.9 Hz), 4.81 (1 H, d, *J* 9.2), 4.93 (1 H, dd, *J* 36.1 and 9.7), 5.38 (1 H, t, *J* 5.7), 7.26–7.79 (18 H, m) and 8.02–8.07 (1 H, m); δ_C (125 MHz, $CDCl_3$, Me_4Si) 25.6, 28.9, 38.4, 42.9, 47.1, 51.6 (d, *J* 27.6), 62.3, 66.7, 104.7 (d, *J* 14.4), 120.0 (2 C), 124.4, 124.9, 125.0 (2 C), 125.2 (2 C), 125.5 (2 C), 125.9, 127.1, 127.5 (2 C), 127.7, 127.8, 130.9, 132.2, 132.7, 133.3, 133.5, 133.5, 135.6, 141.3 (2 C), 143.7, 143.8, 147.9, 158.0 (d, *J* 262.0), 163.0 and 177.0; δ_F (125 MHz, $CDCl_3$, $CFCl_3$) −120.8; HRMS (FAB), *m/z* calcd for $C_{40}H_{35}FN_3O_8S$ ([M − H]$^-$) 736.2134, found: 736.2137.

Peptide synthesis

The protected linear peptides **20a,b** were constructed on H–Gly–(2-Cl)Trt resin (0.8 mmol g^{-1}, 38 mg, 0.03 mmol). *t*-Bu was employed for Tyr side-chain protection. Fmoc-protected amino acids (0.3 mmol) were coupled by using DIC (0.046 cm^3, 0.3 mmol) and HOBt·H_2O (46 mg, 0.3 mmol) in DMF. Coupling of EADI **14** (33mg, 0.045 mmol) was carried out with HOAt (6.3 mg, 0.045 mmol), HATU (17 mg, 0.045 mmol) and (*i*-Pr)$_2$NEt (0.009 cm^3, 0.045 mmol). Completion of each coupling reaction was ascertained using the Kaiser ninhydrin test. The Fmoc-protecting group was removed by treating the resin with a DMF/piperidine solution (80/20, v/v).

***cyclo*(−D−Tyr−Arg−Ψ[(*E*)-CH=CH]−Arg−Nal−Gly−)·2TFA (3E).** The obtained resin **20a** was treated with HFIP/CH_2Cl_2 (2/8, 15 cm^3) at room temperature for 2 h. After removal of the resin by filtration, the filtrate solution was concentrated under reduced pressure to give a crude protected peptide **21a**. To a mixture of **21a** and $NaHCO_3$ (21 mg, 0.25 mmol) in DMF (20 cm^3) was added DPPA (0.0270 cm^3, 0.13 mmol) at −40 °C. The mixture was stirred for 66 h with warming to room temperature and then filtered. The filtrate was concentrated under reduced pressure to give the protected cyclic peptide **22a**. The peptide **22a** was treated with 1 M TMSBr/thioanisole in TFA (10 cm^3) in the presence of *m*-cresol and 1,2-ethandithiol (0.117 cm^3) for 6 h at 0 °C. The mixture was poured into ice-cold dry Et_2O. The resulting powder was collected and washed three times with ice-cold dry Et_2O. To a stirred solution of the precipitant **23a** in DMF (1 cm^3) were added (*i*-Pr)$_2$NEt (0.014 cm^3, 0.08 mmol) and 1*H*-pyrazole-1-carboxamidine·HCl (12 mg, 0.04 mmol), and the mixture was stirred at room temperature for 60 h. After concentration under reduced pressure, purification by preparative HPLC gave the bis-trifluoroacetate salt of the title peptide **3E** (1.9 mg, 9% yield based on H–Gly–(2-Cl)Trt resin, >98% purity by HPLC analysis) as a colorless freeze-dried powder: HRMS (FAB), *m/z* calcd for $C_{37}H_{49}N_{10}O_5$ ([M+H]$^+$) 713.3882, found 713.3886.

***cyclo*(−D−Tyr−Arg−Arg−Ψ[(*Z*)-CF=CH]−Nal−Gly−)·2TFA (4F).** Cyclic peptide **4F** was synthesized by a procedure identical with that described for the synthesis of **3E**. The protected peptide **22b** (32.0 mg, 0.0270 mmol) was treated with aqueous TFA/H_2O (95/5, 10 cm^3) for 3 h. Concentration under reduced pressure gave an oily residue. To a solution of the residue in DMF (8 cm^3) were added 2-mercaptoethanol (0.0191 cm^3, 0.270 mmol) and DBU (0.0809 cm^3, 0.540 mmol), and the mixture was stirred at 50 °C for 2.5 h. After concentration under reduced pressure, the residue **23b** was treated with Et_3N (0.112 cm^3, 0.810 mmol) and 1*H*-pyrazole-1-carboxamidine·HCl (39.6 mg, 0.270 mmol) in DMF (2 cm^3). After concentration under reduced pressure, purification by preparative HPLC gave the bis-trifluoroacetate salt of the title peptide **4F** (3.6 mg, 6% yield based on H–Gly–(2-Cl)Trt resin, 89% purity by HPLC analysis): HRMS (FAB), *m/z* calcd for $C_{37}H_{48}FN_{10}O_5$ ([M+H]$^+$) 731.3788, found 731.3796.

[^{125}I]-SDF-1 binding and displacement

Membrane extracts were prepared from CHO-K1 cell lines expressing either CXCR4 or CXCR7. For ligand binding, 0.050 cm^3 of the inhibitor, 0.025 cm^3 of [^{125}I]-SDF-1α (0.3 nM, Perkin-Elmer Life Sciences) and 0.025 cm^3 of the membrane/beads mixture [CXCR4: 7.5 μg well^{-1} of membrane, 0.5 mg well^{-1} of PVT WGA beads (Amersham); CXCR7: 3 μg well^{-1} of membrane, 0.25 mg well^{-1} of PVT-PEI type A beads (Amersham)] in assay buffer (25 mM HEPES pH 7.4, 1 mM $CaCl_2$, 5 mM $MgCl_2$, 140 mM NaCl, 250 mM sucrose, 0.5% BSA) were incubated in the wells of an Optiplate places (Perkin-Elmer Life Sciences) at room temperature for 1 h. The bound radioactivity was counted for 1 min well^{-1} in a TopCount (Packard). Inhibitory activity of the test compounds was determined based on the inhibition of [^{125}I]-SDF-1 binding to the receptors (IC_{50}).

Determination of anti-HIV activity

The peptide sensitivity of three HIV-1 strains was determined by the MAGI assay with some modifications.[22] Briefly, the target cells (HeLa-CD4/CCR5-LTR-β-gal; 10^4 cells well^{-1}) were plated in 96-well flat microtiter culture plates. On the following day,

the cells were inoculated with the HIV-1 (60 MAGI U/well, giving 60 blue cells after 48 h of incubation) and cultured in the presence of various concentrations of the drugs in fresh medium. Forty-eight hours after viral exposure, all the blue cells stained with X-Gal (5-bromo-4-chloro-3-indolyl-β-D-galactopyranoside) were counted in each well. The activity of test compounds was determined as the concentration that blocked HIV-1 replication by 50% (50% effective concentration [EC_{50}]).

Acknowledgements

This work was supported by Grants-in-Aid for Scientific Research from MEXT, Japan, and Health and Labour Science Research Grants (Research on HIV/AIDS). T.N. and K.T. are grateful for the JSPS Research Fellowships for Young Scientists. We are grateful to Prof. Hirokazu Tamamura and Mr. Tomohiro Tanaka for helpful discussions.

References

1 (*a*) M. Loetscher, T. Geiser, T. O'Reilly, R. Zwahlen, M. Baggiolini and B. Moser, *J. Biol. Chem*, 1994, **269**, 232–237; (*b*) B. J. Rollins, *Blood*, 1997, **90**, 909–928.

2 (*a*) T. Nagasawa, S. Hirota, K. Tachibana, N. Takakura, S. Nishikawa, Y. Kitamura, N. Yoshida, H. Kikutani and T. Kishimoto, *Nature*, 1996, **382**, 635–638; (*b*) K. Tachibana, S. Hirota, H. Iizasa, H. Yoshida, K. Kawabata, Y. Kataoka, Y. Kitamura, K. Matsushima, N. Yoshida, S. Nishikawa, T. Kishimoto and T. Nagasawa, *Nature*, 1998, **393**, 591–594.

3 C. C. Bleul, R. C. Fuhlbrigge, J. M. Casanovas, A. Aiuti and T. A. Springer, *J. Exp. Med.*, 1996, **184**, 1101–1109.

4 (*a*) Y. Zhu, Y. Yu, X. C. Zhang, T. Nagasawa, J. Y. Wu and Y. Rao, *Nat. Neurosci.*, 2002, **5**, 513–720; (*b*) R. K. Stumm, C. Zhou, T. Ara, F. Lazarini, M. Dubois-Dalcq, T. Nagasawa, V. Hollt and S. Schulz, *J. Neurosci.*, 2003, **23**, 5123–5130.

5 (*a*) A. Müller, B. Homey, H. Soto, N. Ge, D. Catron, M. E. Buchanan, T. Mcclanahan, E. Murphy, W. Yuan, S. M. Wagner, J. L. Barrera, A. Mohar, E. Verástegui and A. Zlotnik, *Nature*, 2001, **410**, 50–56; (*b*) J. A. Burger, M. Burger and T. J. Kipps, *Blood*, 1999, **94**, 3658–3667.

6 Y. Feng, C. C. Broder, P. E. Kennedy and E. A. Berger, *Science*, 1996, **272**, 872–877.

7 T. Nanki, K. Hayashida, H. S. EI-Gabalawy, S. Suson, K. Shi, H. J. Girschick, S. Yavuz and P. E. Lipsky, *J. Immunol.*, 2000, **165**, 6590–6598.

8 (*a*) T. Murakami, T. Nakajima, Y. Koyanagi, K. Tachibana, N. Fujii, H. Tamamura, N. Yoshida, M. Waki, A. Matsumoto, O. Yoshie, T. Kishimoto, N. Yamamoto and T. Nagasawa, *J. Exp. Med.*, 1997, **186**, 1389–1393; (*b*) D. Schols, S. Struyf, J. Van Damme, J. A. Este, G. Henson and E. De Clercq, *J. Exp. Med.*, 1997, **186**, 1383–1388; (*c*) G. A. Donzella, D. Schols, S. W. Lin, J. A. Este, K. A. Nagashima, P. J. Maddon, G. P. Allaway, T. P. Sakmar, G. Henson, E. De Clercq and J. P. Moore, *Nat. Med.*, 1998, **4**, 72–77; (*d*) B. J. Doranz, K. Grovit-Ferbas, M. P. Sharron, S.-H. Mao, M. Bidwell Goetz, E. S. Daar, R. W. Doms and W. A. O'Brien, *J. Exp. Med.*, 1997, **186**, 1395–1400; (*e*) O. M. Z. Howard, J. J. Oppenheim, M. G. Hollingshead, J. M. Covey, J. Bigelow, J. J. McCormack, R. W. Buckheit Jr., D. J. Clanton, J. A. Turpin and W. G. Rice, *J. Med. Chem.*, 1998, **41**, 2184–2193.

9 For recent reviews, see:(*a*) H. Shim, S. Oishi and N. Fujii, *Semin. Cancer Biol.*, 2009, **19**, 123–134; (*b*) E. De Clercq, *Biochem. Pharmacol.*, 2009, **77**, 1655–1664.

10 (*a*) H. Tamamura, A. Omagari, S. Oishi, T. Kanamoto, N. Yamamoto, S. C. Peiper, H. Nakashima, A. Otaka and N. Fujii, *Bioorg. Med. Chem. Lett.*, 2000, **10**, 2633–2637; (*b*) H. Tamamura, Y. Sugioka, A. Odagaki, A. Omagari, Y. Kan, S. Oishi, H. Nakashima, N. Yamamoto, S. C. Peiper, A. Hamanaka, A. Otaka and N. Fujii, *Bioorg. Med. Chem. Lett.*, 2001, **11**, 359–362.

11 N. Fujii, S. Oishi, K. Hiramatsu, T. Araki, S. Ueda, H. Tamamura, A. Otaka, S. Kusano, S. Terakubo, H. Nakashima, J. A. Broach, J. O. Trent, Z. Wang and S. C. Peiper, *Angew. Chem., Int. Ed.*, 2003, **42**, 3251–3253.

12 (*a*) H. Tamamura, A. Esaka, T. Ogawa, T. Araki, S. Ueda, Z. Wang, J. O. Trent, H. Tsutsumi, H. Masuno, H. Nakashima, N. Yamamoto, S. C. Peiper, A. Otaka and N. Fujii, *Org. Biomol. Chem.*, 2005, **3**, 4392–4394; (*b*) T. Tanaka, H. Tsutsumi, W. Nomura, Y. Tanabe, N. Ohashi, A. Esaka, C. Ochiai, J. Sato, K. Itotani, T. Murakami, K. Ohba, N. Yamamoto, N. Fujii and H. Tamamura, *Org. Biomol. Chem.*, 2008, **6**, 4374–4377; (*c*) T. Tanaka, W. Nomura, T. Narumi, A. Esaka, S. Oishi, N. Ohashi, K. Itotani, B. J. Evans, Z. Wang, S. C. Peiper, N. Fujii and H. Tamamura, *Org. Biomol. Chem.*, 2009, **7**, 3805–3809.

13 H. Tamamura, T. Araki, S. Ueda, Z. Wang, S. Oishi, A. Esaka, J. O. Trent, H. Nakashima, N. Yamamoto, S. C. Peiper, A. Otaka and N. Fujii, *J. Med. Chem.*, 2005, **48**, 3280–3289.

14 S. Ueda, S. Oishi, Z. Wang, T. Araki, H. Tamamura, J. Cluzeau, H. Ohno, S. Kusano, H. Nakashima, J. O. Trent, S. C. Peiper and N. Fujii, *J. Med. Chem.*, 2007, **50**, 192–198.

15 H. Tamamura, K. Hiramatsu, S. Ueda, Z.-X. Wang, S. Kusano, S. Terakubo, J. O. Trent, S. C. Peiper, N. Yamamoto, H. Nakashima, A. Otaka and N. Fujii, *J. Med. Chem.*, 2005, **48**, 380–391.

16 For some recent exapmles of unsubstituted alkene dipeptide isosteres, see: (*a*) S. Oishi, H. Tamamura, M. Yamashita, N. Hamanaka, A. Otaka and N. Fujii, *J. Chem. Soc., Perkin Trans. 1*, 2001, 2445–2451; (*b*) M. M. Vasbinder, E. R. Jarvo and S. J. Miller, *Angew. Chem., Int. Ed.*, 2001, **40**, 2824–2827; (*c*) M. M. Vasbinder and S. J. Miller, *J. Org. Chem.*, 2002, **67**, 6240–6242; (*d*) N. G. Bandur, K. Harms and U. Koert, *Synlett*, 2005, 773–776; (*e*) C. L. Jenkins, M. M. Vasbinder, S. J. Miller and R. T. Raines, *Org. Lett.*, 2005, **7**, 2619–2622; (*f*) D. Wiktelius and K. Luthman, *Org. Biomol. Chem.*, 2007, **5**, 603–605; (*g*) N. G. Bandur, K. Harms and U. Koert, *Synlett*, 2007, 99–102, and references cited therein.

17 For some recent exapmles of fluoroalkene dipeptide isosteres, see: (*a*) A. Otaka, J. Watanabe, A. Yukimasa, Y. Sasaki, H. Watanabe, T. Kinoshita, S. Oishi, H. Tamamura and N. Fujii, *J. Org. Chem.*, 2004, **69**, 1634–1645; (*b*) P. Van der Veken, K. Senten, I. Kertèsz, I. D. Meester, A.-M. Lambeir, M.-B. Maes, S. Scharpè, A. Haemers and K. Augustyns, *J. Med. Chem.*, 2005, **48**, 1768–1780; (*c*) Y. Nakamura, M. Okada, A. Sato, H. Horikawa, M. Koura, A. Saito and T. Taguchi, *Tetrahedron*, 2005, **61**, 5741–5753; (*d*) S. Sano, Y. Kuroda, K. Saito, Y. Ose and Y. Nagao, *Tetrahedron*, 2006, **62**, 11881–11890; (*e*) T. Narumi, A. Niida, K. Tomita, S. Oishi, A. Otaka, H. Ohno and N. Fujii, *Chem. Commun.*, 2006, 4720–4722; (*f*) G. Dutheuil, S. Couve-Bonnaire and X. Pannecoucke, *Angew. Chem., Int. Ed.*, 2007, **46**, 1290–1292; (*g*) T. Narumi, K. Tomita, E. Inokuchi, K. Kobayashi, S. Oishi, H. Ohno and N. Fujii, *Org. Lett.*, 2007, **9**, 3465–3468; (*h*) C. Lamy, J. Hofmann, H. Parrot-Lopez and P. Goekjian, *Tetrahedron Lett.*, 2007, **48**, 6177–6180; (*i*) T. Narumi, K. Tomita, E. Inokuchi, K. Kobayashi, S. Oishi, H. Ohno and N. Fujii, *Tetrahedron*, 2008, **64**, 4332–4346; (*j*) Y. Yamaki, A. Shigenaga, K. Tomita, T. Narumi, N. Fujii and A. Otaka, *J. Org. Chem.*, 2009, **74**, 3272–3277; (*k*) Y. Yamaki, A. Shigenaga, J. Li, Y. Shimohigashi and A. Otaka, *J. Org. Chem.*, 2009, **74**, 3278–3285; (*l*) S. Oishi, H. Kamitani, Y. Kodera, K. Watanabe, K. Kobayashi, T. Narumi, K. Tomita, H. Ohno, T. Naito, E. Kodama, M. Matsuoka and N. Fujii, *Org. Biomol. Chem.*, 2009, **7**, 2872–2877.

18 For some recent examples of tri- or tetrasubstituted alkene isosteres, see: (*a*) S. Oishi, T. Kamano, A. Niida, Y. Odagaki, N. Hamanaka, M. Yamamoto, K. Ajito, H. Tamamura, A. Otaka and N. Fujii, *J. Org. Chem.*, 2002, **67**, 6162–6173; (*b*) S. Oishi, K. Miyamoto, A. Niida, M. Yamamoto, K. Ajito, H. Tamamura, A. Otaka, Y. Kuroda, A. Asai and N. Fujii, *Tetrahedron*, 2006, **62**, 1416–1424; (*c*) J. Xiao, B. Weisblum and P. Wipf, *Org. Lett.*, 2006, **8**, 4731–4734; (*d*) N. Dai, X. J. Wang and F. A. Etzkorn, *J. Am. Chem. Soc.*, 2008, **130**, 5396–5397.

19 (*a*) P. Wipf, T. C. Henninger and S. J. Geib, *J. Org. Chem.*, 1998, **63**, 6088–6089; (*b*) J. Xiao, B. Weisblum and P. Wipf, *J. Am. Chem. Soc.*, 2005, **127**, 5742–5743; (*c*) P. Wipf, J. Xiao and S. J. Geib, *Adv. Synth. Catal.*, 2005, **347**, 1605–1613; (*d*) K. Kobayashi, T. Narumi, S. Oishi, H. Ohno and N. Fujii, *J. Org. Chem.*, 2009, **74**, 4626–4629.

20 S. Couve-Bonnaire, D. Cahard and X. Pannecoucke, *Org. Biomol. Chem.*, 2007, **5**, 1151–1157, and references cited therein.

21 S. Oishi, R. Masuda, B. Evans, S. Ueda, Y. Goto, H. Ohno, A. Hirasawa, G. Tsujimoto, Z. Wang, S. C. Peiper, T. Naito, E. Kodama, M. Matsuoka and N. Fujii, *ChemBioChem*, 2008, **9**, 1154–1158.

22 (*a*) E. Kodama, S. Kohgo, K. Kitano, H. Machida, H. Gatanaga, S. Shigeta and M. Matsuoka, *Antimicrob. Agents Chemother.*, 2001, **45**, 1539–1546; (*b*) Y. Maeda, D. J. Venzon and H. Mitsuya, *J. Infect. Dis.*, 1998, **177**, 1207–1213.

Antiviral Research 80 (2008) 71–76

Contents lists available at ScienceDirect

Antiviral Research

journal homepage: www.elsevier.com/locate/antiviral

Novel screening systems for HIV-1 fusion mediated by two extra-virion heptad repeats of gp41

Hiroki Nishikawa[a], Eiichi Kodama[b,*], Ayako Sakakibara[b], Ayako Fukudome[b], Kazuki Izumi[b], Shinya Oishi[a], Nobutaka Fujii[a], Masao Matsuoka[b]

[a] Graduate School of Pharmaceutical Sciences, Kyoto University, Sakyo-ku, Kyoto 606-8501, Japan
[b] Laboratory of Virus Immunology, Institute for Virus Research, Kyoto University, Sakyo-ku, Kyoto 606-8507, Japan

ARTICLE INFO

Article history:
Received 12 November 2007
Accepted 5 May 2008

Keywords:
HIV-1
Gp41
Fusion
ELISA
Screening
Alkaline phosphatase

ABSTRACT

Entry of human immunodeficiency virus type 1 (HIV-1) into target cells is mediated by its envelope protein gp41 through membrane fusion. Interaction of two extra-virion heptad repeats (HRs) in the gp41 plays a pivotal role in the fusion, and its inhibitor, enfuvirtide (T-20), blocks HIV-1 entry. To identify agents that block HIV-1 fusion, two screening methods based on detection and quantification by the enzyme-linked immunosorbent assay (ELISA) principle have been established. One method uses an alkaline phosphatase (ALP)-conjugated antibody (Ab-ELISA) and the other uses an ALP-fused HR (F-ELISA) to detect and quantify the interaction of the two HRs. The F-ELISA was more simple and rapid, since no ALP-conjugated antibody reaction was required. Both ELISAs detected all the fusion inhibitors tested except for T-20. Interaction of the two HRs was observed in both ELISAs, even in the presence of 10% dimethyl sulfoxide. Ab-ELISA performed best in a pH ranging from 6 to 8, while F-ELISA performed best at a pH ranging from 7 to 8. These results indicate that both established ELISAs are suitable for the identification of HIV-1 fusion inhibitors.

1. Introduction

Combination chemotherapy has been widely used and reduces the mortality caused by HIV-1 infection. During prolonged therapy, however, in some patients, such efficacy is attenuated by the emergence of drug-resistant variants (Calmy et al., 2004). Moreover, combination chemotherapy occasionally induces various adverse effects and may also increase the costs of the therapy. Therefore, development of novel anti-HIV-1 drugs that suppress replication of resistant variants, and are less toxic and less cost is urgently needed.

There are at least two approaches to controlling replication of resistant variants and/or to reducing unfavorable adverse effects induced by the therapy. One approach is the development of anti-HIV-1 drugs which inhibit new targets such as viral integrase (Hazuda et al., 2004) or cellular receptors such as CCR5 (Tagat et al., 2004). Actually, an integrase inhibitor, raltegravir (Grinsztejn et al., 2007), and a CCR5 antagonist, maraviroc (Fätkenheuer et al., 2005) have been approved for clinical application. The other is the development or modification of current drugs that inhibit well-established targets, to make them effective against resistant variants while reducing adverse side-effects. In this study, we focus on the recently established and promising target of virus–cell membrane fusion.

The mechanism of virus–cell membrane fusion has already been disclosed (Eckert and Kim, 2001). Briefly, one of the HIV-1 envelope glycoproteins, gp120, binds to the host cell receptor CD4 and CXCR4 or CCR5, and then, another membrane-spanning protein gp41 in trimer anchors itself to the host cell membrane. After anchoring, heptad repeats 1 and 2 (HR1 and HR2), which are two extra-virion α-helical regions in the gp41, form an anti-parallel 6-helical bundle and lead to fusion of HIV-1 with the host cell membrane. On the basis of this molecular mechanism, compounds which prevent 6-helical bundle formation will be potential HIV-1 fusion inhibitors. Enfuvirtide (T-20) is the first peptide approved and used against HIV-1 variants that are refractory to the effect of reverse transcriptase and protease inhibitors (Lalezari et al., 2003; Lazzarin et al., 2003). Previously, we and others have developed novel potent fusion inhibitors, in the form of gp41 HR2-derived peptides (Bewley et al., 2002; Otaka et al., 2002; Root et al., 2001) (Fig. 1) and small molecules (Cai and Gochin, 2007; Frey et al., 2006). However, no fusion inhibitors, except for T-20, have been approved for clinical use. To screen further potential fusion inhibitors, we have established two simple, rapid and reproducible

* Corresponding author. Tel.: +81 75 751 3986; fax: +81 75 751 3986.
E-mail address: ekodama@virus.kyoto-u.ac.jp (E. Kodama).

0166-3542/$ – see front matter © 2008 Elsevier B.V. All rights reserved.
doi:10.1016/j.antiviral.2008.05.006

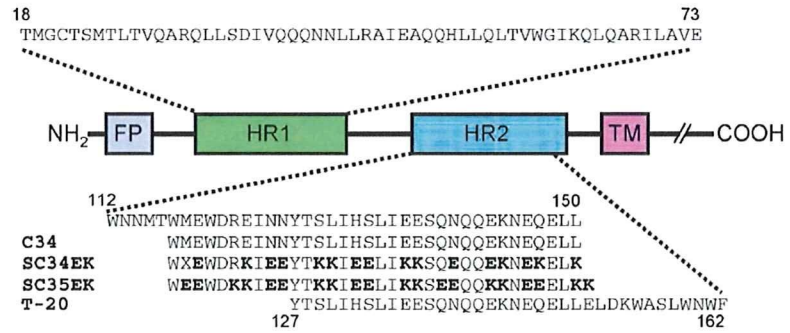

Fig. 1. Schematic view of gp41. The locations of the fusion peptide (FP), N-terminal heptad repeat region (HR1), C-terminal heptad repeat region (HR2), transmembrane domain (TM) and amino acid sequence of HR1, HR2, T-20, C34 and its derivatives (Otaka et al., 2002) are shown. The residue numbers of each peptide correspond to their positions in the envelope protein gp41 of HIV-1 NL4-3 clone. Representative regions of HR1 and HR2 used in this study are defined by the amino acids 18–73 and 112–150, respectively, and designated as MBP-HR1- and GST-HR2- or TRX-ALP-HR2-fused protein as described in Section 2. The X in SC34EK indicates an artificial amino acid norleucine instead of methionine, to avoid oxidation of the methionine residue.

in vitro screening systems using the enzyme-linked immunosorbent assay (ELISA).

2. Materials and methods

2.1. Antiviral agents

The peptide-based fusion inhibitors were synthesized as described previously (Otaka et al., 2002), and their sequences are shown in Fig. 1. CCR5 antagonist TAK-779 (Baba et al., 1999) was provided by Takeda Pharmaceutical Company Ltd. (Osaka, Japan) through an AIDS research and reference reagent program. CXCR4 antagonist AMD-3100 (De Clercq et al., 1994) was provided by S. Shigeta (Fukushima Medical University, Fukushima, Japan). Adsorption inhibitor dextran sulfate MW 5000, DS-5000 (Baba et al., 1988) was purchased from Sigma (St. Louis, MO).

2.2. Protein expression and purification

A DNA fragment of the alkaline phosphatase (ALP) coding region without its secretory signal sequence, corresponding to amino acids 22–471 (Dodt et al., 1986; Kikuchi et al., 1981), was amplified by PCR from the *E. coli* JM109 genome (K12 strain; GenBank accession number: U00096). The amplified ALP region was ligated into the pET32a vector (Novagen, Madison, WI) to create pET32-ALP, a thioredoxin (TRX)-ALP fusion construct. A DNA fragment coding the HR1 region of HIV-1 gp41, amino acid positions 18–73, was amplified by PCR from an HIV-1 molecular clone pNL4-3 (GenBank accession number: AF324493). The amplified HR1 region was ligated into the pMAL-C2 vector (New England Biolabs, Ipswich, MA) to express HR1 with maltose-binding protein (MBP) as a tag, designated pMAL-HR1. The HR2 region, gp41 amino acid positions 112–150, was also amplified and ligated into both the pGEX-5X vector (GE Healthcare, Buckinghamshire, UK) and the pET32-ALP construct to express HR2 fusion protein with glutathione *S*-transferase (GST) and TRX-ALP, designated pGEX-HR2 and pET32-ALP-HR2, respectively. All vectors were verified by DNA sequencing and transformed into *E. coli* BL21-CodonPlus (DE3)-RIL strain (Stratagene, La Jolla, CA) for bacterial expression. The expressed MBP-HR1, GST-HR2 and TRX-ALP-HR2 proteins were purified by Amylose Resin (New England Biolabs), Glutathione Sepharose 4B (GE Healthcare) and Ni-NTA Agarose (Qiagen, Valencia, CA), respectively, according to the Manufacturers' recommended protocols. Purity was determined by SDS–PAGE and concentration by the Bradford protein assay (Bio-Rad, Hercules, CA).

2.3. Indirect detection of interaction of HR1 and HR2 (Ab-ELISA) (Fig. 2A)

Fifty nanomolar MBP-HR1 dissolved in 50 mM sodium carbonate buffer (pH 9.4) was coated on a 96-well ELISA plate (Costar, Cambridge, MA) by incubation at 4 °C for 8 h. After washing three times with PBS containing 0.025% Tween 20 (T-PBS) (pH 7.4), the plate was blocked using bovine serum albumin (BSA) at a concentration of 1 mg/ml in T-PBS at 4 °C for 2.5 h, and then washed again as described above. The MBP-HR1 on the plate was allowed to bind GST-HR2 (50 nM) by incubation at 37 °C for 1.5 h in the presence or absence of various concentrations of compounds for testing. After washing, binding of GST-HR2 was detected by using alkaline phosphatase (ALP)-conjugated anti-GST antibody (Sigma) in 1:2000 dilution at 4 °C for 1 h, then washed as before, prior to the addition of phosphatase substrate 5-bromo-4-chloro-3-indolyl phosphate (BCIP) (BluePhos Microwell Phosphatase Substrate; KPL, Gaithersburg, MD). After incubating at room temperature for 30 min, absorbance at 595 nm was measured by a plate reader (model 3550, Bio-Rad).

2.4. Direct detection of interaction of HR1 and HR2 (F-ELISA) (Fig. 2D)

All procedures were performed as described above, except that TRX-ALP-HR2 (50 nM) was used in place of GST-HR2, with binding directly detected by BluePhos Microwell Phosphatase Substrate without the interaction of ALP-conjugated anti-GST antibody.

2.5. Anti-HIV activity

Anti-HIV-1 activity was determined by the multinuclear activation of a galactosidase indicator (MAGI) assay as described previously (Kimpton and Emerman, 1992; Kodama et al., 2001). Briefly, the MAGI cells (10^4 cells/well) were seeded in flat bottom 96-well microtitre plates. The following day, the cells were inoculated with HIV-1 and cultured in the presence of various concentrations of inhibitors in fresh medium. After 48 h incubation, all the blue cells stained with 5-bromo-4-chloro-3-indolyl-β-D-galactopyranoside (X-gal) in each well were counted.

3. Results

3.1. Establishment of ELISA

To establish a novel assay system representing the specific interaction of HR1 and HR2 regions of the HIV-1 gp41 protein, a

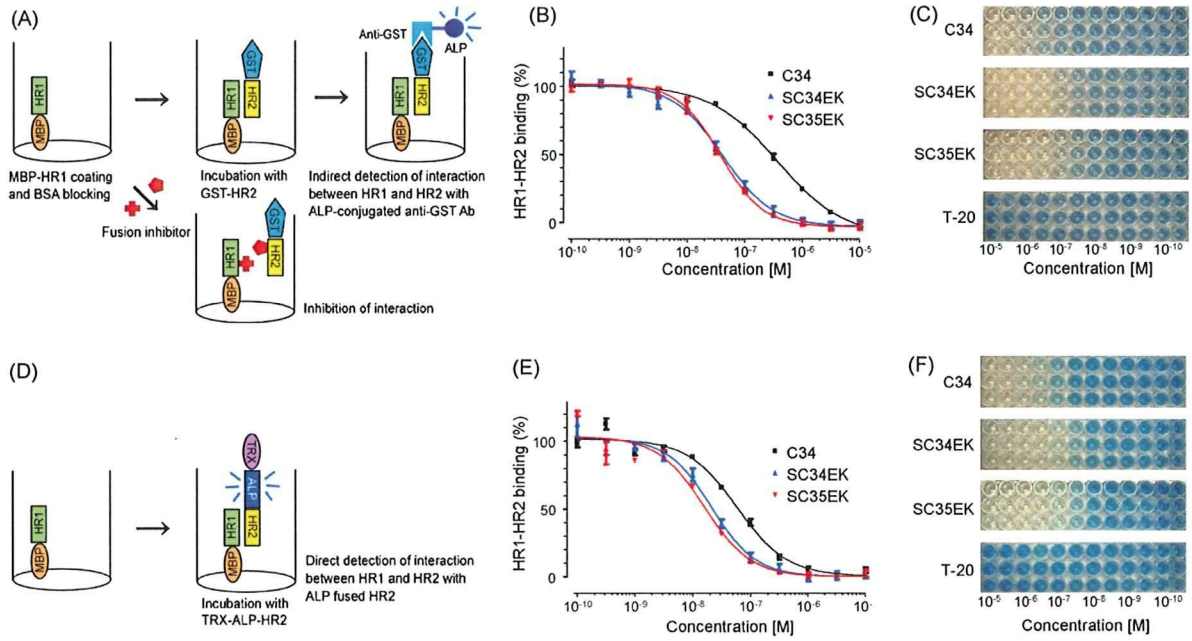

Fig. 2. Flow chart of the established ELISA systems (A and D) and the inhibitory effects of peptide-based fusion inhibitors determined by these systems (B, C, E and F). The schemes of Ab-ELISA and F-ELISA are shown. In Ab-ELISA (A), GST-HR2 interacts with MBP-HR1 on the ELISA plate, and the amounts of GST-HR2 are quantified by using ALP-conjugated anti-GST antibody and ALP substrate. In the presence of fusion inhibitors, GST-HR2 cannot interact with MBP-HR1, resulting in no ALP activity. In F-ELISA (D), ALP-fused HR2 protein enables the detection of the interaction of HR2 directly without ALP-conjugated anti-GST antibody. Inhibition curves of binding by Ab-ELISA (B) and F-ELISA (E) at peptide concentrations 10^{-10} to 10^{-5} M are illustrated. The actual appearance of ELISA plates observed in Ab-ELISA (C) and F-ELISA (F) is shown.

simple ELISA was first established with ALP-conjugated antibody (Ab-ELISA) as shown in Fig. 2A. MBP-HR1 was coated onto a 96-well ELISA plate. After blocking with BSA, GST-HR2 solution was added to the MBP-HR1 coated well. Using ALP-conjugated anti-GST antibody, the interaction of HR1 and HR2 was colorimetrically measured by a plate reader. Agents that block the interaction of HR2 with HR1 can reduce optical density at 595 nm (OD_{595}). The period for efficient coating of MBP-HR1 to the plate was measured by detection of ALP-conjugated anti-MBP antibody. After 8 h and up to 24 h little increase in efficiency of MBP-HR1 coating was observed (data not shown). When coating and blocking were performed prior to the assay, total time of the procedure, excluding washing, was only 3 h.

Prior to evaluation of fusion inhibitors, we examined interaction of GST-HR2 with the MBP-HR1 coating. We first coated MBPs with or without HR1 at a concentration of 50 nM, incubated them with various concentrations of GST-HR2, and then detected bound GST-HR2 with anti-GST antibody. GST-HR2 interacted with MBP-HR1 in a dose-dependent manner, at least up to 100 μM and provided sufficient OD_{595} values, over 1.0 (Fig. 3). Thus, 50 nM of GST-HR2 was used for further experiments.

Next, we modified the Ab-ELISA by using ALP-fused HR2 instead of GST-HR2 in the reaction with coated MBP-HR1, as shown in Fig. 2D (F-ELISA). The ALP-fused HR2 enabled us to directly detect the HR1 and HR2 interaction without the antibody reaction step, thus providing an even more rapid and simple procedure than the Ab-ELISA which uses ALP-conjugated antibody for detection. The total time required for the F-ELISA, excluding coating and blocking, was approximately 2 h. These results demonstrate that the ELISA systems detect the interaction of HR1 and HR2 interaction, enables the screening of potential fusion inhibitors without the need for infectious HIV-1 material, and is both simple and rapid.

3.2. Inhibitory effect of HR2-derived peptides and other entry inhibitors

The efficacy of the fusion inhibitory peptides C34, SC34EK and SC35EK and other compounds was determined by both Ab-ELISA (Fig. 2A) and F-ELISA (Fig. 2D). Both ELISAs only detected the activities of these three fusion inhibitory peptides, but not of other entry inhibitors (Table 1). The inhibitory effects of these peptide fusion inhibitors were reproducible and displayed a sigmoidal dose-dependent curve (Fig. 2B and E). These results suggested that our established ELISAs were specific for the interaction between HR1 and HR2 in the fusion process. Higher sensitivities for peptides tested were obtained by F-ELISA compared with those by Ab-ELISA (Table 1). However, compared with the MAGI assay, sensitivities of both ELISAs were between 14- and 50-fold lower. Neither ELISA technique was able to detect the inhibitory effect of T-20, which

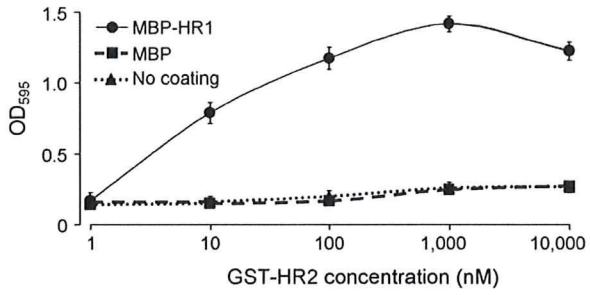

Fig. 3. The binding efficacy of GST-HR2. Fifty nanomolars of MBP-HR1 (circle), MBP (square) and mock (triangle with broken line) were coated on the plate. Various concentrations of GST-HR2 were added and incubated at 37 °C for 1.5 h. Bound GST-HR2 was detected with ALP-conjugated anti-GST antibody by measuring the optical density at 595 nm (OD_{595}).

Table 1
The efficacy of HR2-derived peptides and other entry inhibitors as determined by Ab-ELISA or F-ELISA and the cell-based MAGI assay

Compounds	EC_{50} (nM)[a]			
	Ab-ELISA[b]	F-ELISA[c]	MAGI[d]	
			NL4-3[e]	BaL[f]
C34[g]	365 ± 43	59 ± 7.7	4.0 ± 0.86	N.D.[h]
SC34EK[g]	41 ± 5.0	21 ± 3.2	1.6 ± 0.61	N.D.
SC35EK[g]	38 ± 3.0	16 ± 2.8	0.35 ± 0.030	N.D.
T-20[g]	>10,000	>10,000	35 ± 17	N.D.
TAK-779	>100,000	>100,000	>100,000	1.85 ± 0.19
AMD-3100	>100,000	>100,000	0.39 ± 0.030	>100,000
DS-5000	>100,000	>100,000	19 ± 6.0	348 ± 46

[a] EC_{50} refers to the concentration of peptides which show 50% inhibition relative to the control.
[b] The amount of binding GST-HR2 measured by ALP-conjugated anti-GST antibody.
[c] Direct detection of HR1 and HR2 interaction without antibody reaction by using ALP-fused HR2 protein.
[d] Multinuclear activation of a galactosidase indicator assay using HeLa CD4-LTR/β-galactosidase indicator cells (Kimpton and Emerman, 1992).
[e] CXCR4 (X4) tropic HIV-1 strain.
[f] CCR5 (R5) tropic HIV-1 strain.
[g] Peptide sequences are shown in Fig. 1.
[h] Not determined.

has anti-fusion activity in vitro and in vivo, even though the gp41 amino acid region 23–58, which is a predictive site for T-20 interaction, is included in the MBP-HR1 fusion protein (Figs. 1 and 2C and F; Table 1). We further examined the effect on T-20 susceptibility of changing the coating and interaction. In this experiment, first GST-HR2 was coated, then exposed to MBP-HR1, and finally detected by anti-MBP antibody. Again C34 and its derivatives were effective, but T-20 was not (data not shown).

3.3. Effect of DMSO concentration and pH

For screening, compounds are frequently dissolved in dimethyl sulfoxide (DMSO). However, high concentrations of DMSO (over 1%) reduced cell viability in the cell-based assay, e.g., MAGI assay. The ELISA systems described here do not require cells, thus should be less influenced by DMSO concentration compared to the MAGI assay. To verify this, we determined the concentration of DMSO that affects the interaction of HR1 and HR2 in our ELISAs. In both the Ab-ELISA and F-ELISA, DMSO concentrations up to 10% did not influence the optical densities to any significant extent (Fig. 4A). At these concentrations, optical densities recorded were less than 20% lower compared to those recorded in the absence of DMSO, indicating that the sensitivities of these tests would be sufficient to screen compounds that are dissolved in reagents containing up to 10% DMSO.

Next, we investigated the effect of pH on detection by ELISA. High concentrations of some compounds that are highly acidic or basic may decrease viability of the cells in cell-based assays. The pH of the reaction buffer was modified by addition of HCl and NaOH as control acidic or basic compounds, respectively. In the F-ELISA, binding of HR1 and HR2 was 2–2.5-fold greater at pH less than 7 than at pH 7.4, while in the Ab-ELISA, the binding was relatively stable at pH 6 (Fig. 4B) and reduction of HR1 and HR2 binding was less than 20%. On the other hand, at basic pH, binding of HR1 and HR2 were relatively stable up to pH 9 in both ELISAs. These results indicate that both systems are less influenced by DMSO concentrations up to 10% and in basic reaction conditions compared to cell-based assays. However, in acidic reaction conditions, interaction of HR1 and HR2 is likely to be overestimated in the F-ELISA.

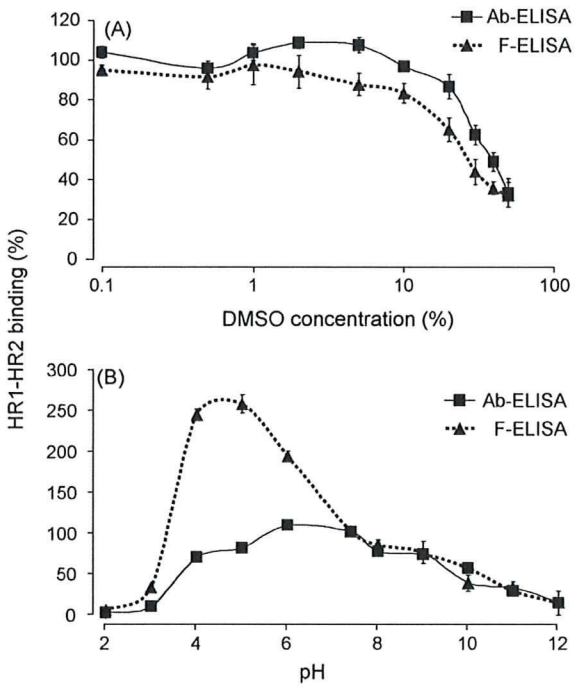

Fig. 4. Effects of DMSO concentration and pH. The effect of DMSO from 0.1 to 50% added to the reaction of HR1 and HR2 is shown (A). Binding is expressed as a percentage of that in the absence of DMSO. Alteration of the pH from 2 to 12 at the HR1 and HR2 reaction was performed by using HCl or NaOH (B). Binding is expressed as a percentage of that at pH 7.4.

4. Discussion

Our newly established ELISA systems successfully detected the HIV-fusion inhibitory activities of C34, a peptide-based fusion inhibitor (Fig. 1), and its derivatives in a dose-dependent manner. However, T-20 lacking the N-terminal 10 amino acids of C34 but containing an additional 12 amino acids in the C-terminal region did not show activity in either of the ELISA systems (Fig. 2; Table 1). T-20 is believed to inhibit 6-helical bundle formation through competition with the physiological HR2 region of gp41. This hypothesis is strongly supported by the introduction of a site of mutations for T-20 resistance in vivo. Variants isolated from T-20 treated patients frequently display mutations in the HR1 region, especially at amino acids 36–45, including D36G/V/S, V38A/E and N43D (Aquaro et al., 2006; Cabrera et al., 2006; Mink et al., 2005; Poveda et al., 2002; Rimsky et al., 1998; Wei et al., 2002) (Fig. 1). Interestingly, amino acid positions 36–45 are also crucial for C34 binding, and some C34 resistant variants also show cross-resistance to T-20 (Nameki et al., 2005). Moreover, our preliminary data in the time course of addition experiments showed that the profile of inhibition is identical between C34 and T-20 (data not shown).

Our designed MBP-HR1 contains the presumed interaction site of T-20 (amino acid positions 23–58), as determined by crystal structure analysis of the N36–C34 complex (Chan et al., 1997) (Fig. 1). However, we failed to detect T-20 inhibitory activity in our ELISA systems (Fig. 2C and F). To the best of our knowledge, there are no reports that describe the potent activity of T-20 in protein- or peptide-based assays (Cai and Gochin, 2007; Huang et al., 2006, 2007; Jiang et al., 1999; Liu et al., 2007; Ryu et al., 1998; Xu et al., 2007).

In this regard, two groups have tried to reveal the mechanism of action of T-20 mainly through physicochemical experiments, with both groups proposing that T-20 may act through the lipid mem-

brane. Jiang et al. has proposed that HR2 peptides have two different functional domains, an HR1-binding domain, and a lipid-binding domain (Liu et al., 2007). C34 contains an HR1-binding sequence but not a lipid-binding domain, while T-20 has only a lipid-binding domain, suggesting that T-20 might be functional only in the presence of lipid membrane. Wexler-Cohen and Shai (2007). also found that the C-terminal region of T-20 which was not included in C34 could be replaced with fatty acid, indicating that T-20 acts through the lipid membrane.

It is possible that MBP hampers the proper conformation of HR1. However, in the 6-helix bundle crystal structure of human T cell leukemia virus type 1 gp21, MBP remained fused to the N-terminal of HR1 (Kobe et al., 1999). Thus, it is unlikely that the inability of HR1 to bind T-20 is due to improper conformation of HR1. Moreover, even synthetic peptides of HR1 and T-20 do not bind each other (Liu et al., 2005).

To date, several peptide-based detection systems have been reported, although they failed to demonstrate T-20 activity. Most of them utilize the NC-1 monoclonal antibody which recognizes discontinuous epitopes presented on the 6-helix complex between N36 and C34 to detect 6-helical conformations (Huang et al., 2006, 2007; Jiang et al., 1999; Liu et al., 2007). It is predicted that this system may not detect the peptide-based fusion inhibitor C34 itself or may not detect C34 derivatives, since the antibody NC-1 was derived from the 6-helix conformation of N36 and C34 peptides. Ryu et al. (1998) also reported similar ELISA systems, but showed an inhibitory effect only for C51 with an EC_{50} value of 1.0 μg/ml (approximately 200 nM). Other groups have reported the development of assay systems using fluorescence resonance energy transfer (FRET) (Cai and Gochin, 2007; Xu et al., 2007). Although FRET requires no coating and washing steps, it seems to be less sensitive compared to our ELISA systems. In fact, EC_{50} values of C34 in the FRET system were described as approximately 5 μM (Xu et al., 2007), while those in our Ab-ELISA and F-ELISA were 365 and 59 nM, respectively (Table 1).

The sensitivities of our ELISA systems were lower than those of the cell-based MAGI assay (Table 1). However, the ELISA systems could detect the interaction between HR1 and HR2 even at a high concentration of DMSO, and in a relatively wide pH range (Fig. 4), indicating their capacity for screening of highly concentrated compounds. Decreased concentrations of MBP-HR1 and GST-HR2 or ALP-HR2 increased the antiviral sensitivity, although this also reduced detection sensitivity of ALP activity. Detection sensitivity could be increased by using a highly sensitive chemiluminescent probe as an alternative to the BCIP substrate we used.

At pH greater than 8, both ELISAs showed decreased optical density, while at pH less than 7, enhanced ALP activity was observed in F-ELISA compared with the neutral pH 7.4 (Fig. 4B). Although we could not elucidate the detailed mechanism at present, even in Ab-ELISA, the optical density was also enhanced by using an acidic buffer in the incubation of GST-HR2 with anti-GST antibody (data not shown). Thus, low pH enhances ALP activity rather than enhancing the interaction of HR1 and HR2. These results indicate that we should take note of this artificial enhancement when acidic compounds are screened by F-ELISA.

Major difference between class I and class II fusion is based upon the structure of the glycoproteins involved in the fusion process. For instance, HIV and FluV utilize alpha-helix structure domains located in gp41 and HA2, respectively. In contrast, Flaviviruses, which fuse through class II, utilize beta-sheet structure domains in E protein. Although both glycoproteins complete fusion with trimer of hairpins (alpha-helix and beta-sheet, respectively), in the pre-fusion state, they form trimers and dimers, for class I and class II, respectively. Moreover, the fusion peptide domain which is directly inserted into target cell membrane, is located at N-terminus and internal loop of the env-protein, for class I and class II, respectively.

At the virus–cell membrane fusion step, the interaction between viral envelope proteins HR1 and HR2 is a common mechanism of class I fusion (Jahn et al., 2003; Schibli and Weissenhorn, 2004). It is expected that establishment of a similar ELISA screening system for other viruses using class I fusion for cell entry, such as influenza virus (Eckert and Kim, 2001), feline immunodeficiency virus (FIV) (Medinas et al., 2002), severe acute respiratory syndrome coronavirus (SARS-CoV) (Bosch et al., 2004) and Ebola virus (Watanabe et al., 2000) is possible. For some highly virulent agents, such as SARS-CoV and Ebola virus, our system will be an extremely useful tool since it does not require infectious material.

In this study, we have developed two novel in vitro assay systems for fusion inhibitors by focusing on the interaction of envelope proteins HR1 and HR2. Hydrophobic pocket in HR1 and tryptophan rich domain in HR2 acting as "pocket" and "knob", respectively, play a key role in the virus–cell membrane fusion process, indicating that these interactions are an attractive target for small molecule fusion inhibitors (Ferrer et al., 1999). C34, GST-HR2 and ALP-TRX-HR2 used in this study contain "knob" region but T-20 does not. The developed systems are also ideal for initial screenings because of low variability and good reproducibility even at high compound concentration, and since they allow for a non-infectious rapid and simple procedure. These assays will be useful for the discovery of novel fusion inhibitors not only of HIV-1, but also of other viruses which utilize the class I fusion mechanism.

Acknowledgements

This work was supported in part by grants for the Promotion of AIDS Research from the Ministry of Health and Welfare and the Ministry of Education, Culture, Sports, Science, and Technology of Japan (E.K. and S.O.); a grant for Research for Health Sciences Focusing on Drug Innovation from The Japan Health Sciences Foundation (E.K., S.O., N.F. and M.M.); and the 21st Century COE program "Knowledge Information Infrastructure for Genome Science" (N.F. and H.N.). H.N. is grateful for the JSPS Research Fellowships for Young Scientists. Appreciation is expressed to Mr. Maxwell Reback (Kyoto University) for reading the manuscript.

References

Aquaro, S., D'Arrigo, R., Svicher, V., Perri, G.D., Caputo, S.L., Visco-Comandini, U., Santoro, M., Bertoli, A., Mazzotta, F., Bonora, S., Tozzi, V., Bellagamba, R., Zaccarelli, M., Narciso, P., Antinori, A., Perno, C.F., 2006. Specific mutations in HIV-1 gp41 are associated with immunological success in HIV-1-infected patients receiving enfuvirtide treatment. J. Antimicrob. Chemother. 58, 714–722.

Baba, M., Nishimura, O., Kanzaki, N., Okamoto, M., Sawada, H., Iizawa, Y., Shiraishi, M., Aramaki, Y., Okonogi, K., Ogawa, Y., Meguro, K., Fujino, M., 1999. A small-molecule, nonpeptide CCR5 antagonist with highly potent and selective anti-HIV-1 activity. Proc. Natl. Acad. Sci. U.S.A. 96, 5698–5703.

Baba, M., Pauwels, R., Balzarini, J., Arnout, J., Desmyter, J., De Clercq, E., 1988. Mechanism of inhibitory effect of dextran sulfate and heparin on replication of human immunodeficiency virus in vitro. Proc. Natl. Acad. Sci. U.S.A. 85, 6132–6136.

Bewley, C.A., Louis, J.M., Ghirlando, R., Clore, G.M., 2002. Design of a novel peptide inhibitor of HIV fusion that disrupts the internal trimeric coiled-coil of gp41. J. Biol. Chem. 277, 14238–14245.

Bosch, B.J., Martina, B.E., Van Der Zee, R., Lepault, J., Haijema, B.J., Versluis, C., Heck, A.J., De Groot, R., Osterhaus, A.D., Rottier, P.J., 2004. Severe acute respiratory syndrome coronavirus (SARS-CoV) infection inhibition using spike protein heptad repeat-derived peptides. Proc. Natl. Acad. Sci. U.S.A. 101, 8455–8460.

Cabrera, C., Marfil, S., García, E., Martinez-Picado, J., Bonjoch, A., Bofill, M., Moreno, S., Ribera, E., Domingo, P., Clotet, B., Ruiz, L., 2006. Genetic evolution of gp41 reveals a highly exclusive relationship between codons 36, 38 and 43 in gp41 under long-term enfuvirtide-containing salvage regimen. AIDS 20, 2075–2080.

Cai, L., Gochin, M., 2007. A novel fluorescence intensity screening assay identifies new low-molecular-weight inhibitors of the gp41 coiled-coil domain of human immunodeficiency virus type 1. Antimicrob. Agents Chemother. 51, 2388–2395.

Calmy, A., Pascual, F., Ford, N., 2004. HIV drug resistance. N. Engl. J. Med. 350, 2720–2721.

Chan, D.C., Fass, D., Berger, J.M., Kim, P.S., 1997. Core structure of gp41 from the HIV envelope glycoprotein. Cell 89, 263–273.
De Clercq, E., Yamamoto, N., Pauwels, R., Balzarini, J., Witvrouw, M., De Vreese, K., Debyser, Z., Rosenwirth, B., Peichl, P., Datema, R., et al., 1994. Highly potent and selective inhibition of human immunodeficiency virus by the bicyclam derivative JM3100. Antimicrob. Agents Chemother. 38, 668–674.
Dodt, J., Schmitz, T., Schäfer, T., Bergmann, C., 1986. Expression, secretion and processing of hirudin in *E. coli* using the alkaline phosphatase signal sequence. FEBS Lett. 202, 373–377.
Eckert, D.M., Kim, P.S., 2001. Mechanisms of viral membrane fusion and its inhibition. Annu. Rev. Biochem. 70, 777–810.
Fätkenheuer, G., Pozniak, A.L., Johnson, M.A., Plettenberg, A., Staszewski, S., Hoepelman, A.I., Saag, M.S., Goebel, F.D., Rockstroh, J.K., Dezube, B.J., Jenkins, T.M., Medhurst, C., Sullivan, J.F., Ridgway, C., Abel, S., James, I.T., Youle, M., van der Ryst, E., 2005. Efficacy of short-term monotherapy with maraviroc, a new CCR5 antagonist, in patients infected with HIV-1. Nat. Med. 11, 1170–1172.
Ferrer, M., Kapoor, T.M., Strassmaier, T., Weissenhorn, W., Skehel, J.J., Oprian, D., Schreiber, S.L., Wiley, D.C., Harrison, S.C., 1999. Selection of gp41-mediated HIV-1 cell entry inhibitors from biased combinatorial libraries of non-natural binding elements. Nat. Struct. Biol. 6, 953–960.
Frey, G., Rits-Volloch, S., Zhang, X.Q., Schooley, R.T., Chen, B., Harrison, S.C., 2006. Small molecules that bind the inner core of gp41 and inhibit HIV envelope-mediated fusion. Proc. Natl. Acad. Sci. U.S.A. 103, 13938–13943.
Grinsztejn, B., Nguyen, B.Y., Katlama, C., Gatell, J.M., Lazzarin, A., Vittecoq, D., Gonzalez, C.J., Chen, J., Harvey, C.M., Isaacs, R.D., 2007. Safety and efficacy of the HIV-1 integrase inhibitor raltegravir (MK-0518) in treatment-experienced patients with multidrug-resistant virus: a phase II randomised controlled trial. Lancet 369, 1261–1269.
Hazuda, D.J., Young, S.D., Guare, J.P., Anthony, N.J., Gomez, R.P., Wai, J.S., Vacca, J.P., Handt, L., Motzel, S.L., Klein, H.J., Dornadula, G., Danovich, R.M., Witmer, M.V., Wilson, K.A., Tussey, L., Schleif, W.A., Gabryelski, L.S., Jin, L., Miller, M.D., Casimiro, D.R., Emini, E.A., Shiver, J.W., 2004. Integrase inhibitors and cellular immunity suppress retroviral replication in rhesus macaques. Science 305, 528–532.
Huang, J.H., Liu, Z.Q., Liu, S., Jiang, S., Chen, Y.H., 2006. Identification of the HIV-1 gp41 core-binding motif—HXXNPF. FEBS Lett. 580, 4807–4814.
Huang, J.H., Yang, H.W., Liu, S., Li, J., Jiang, S., Chen, Y.H., 2007. The mechanism by which molecules containing the HIV gp41 core-binding motif HXXNPF inhibit HIV-1 envelope glycoprotein-mediated syncytium formation. Biochem. J. 403, 565–571.
Jahn, R., Lang, T., Südhof, T.C., 2003. Membrane fusion. Cell 112, 519–533.
Jiang, S., Lin, K., Zhang, L., Debnath, A.K., 1999. A screening assay for antiviral compounds targeted to the HIV-1 gp41 core structure using a conformation-specific monoclonal antibody. J. Virol. Methods 80, 85–96.
Kikuchi, Y., Yoda, K., Yamasaki, M., Tamura, G., 1981. The nucleotide sequence of the promoter and the amino-terminal region of alkaline phosphatase structural gene (phoA) of *Escherichia coli*. Nucl. Acids Res. 9, 5671–5678.
Kimpton, J., Emerman, M., 1992. Detection of replication-competent and pseudotyped human immunodeficiency virus with a sensitive cell line on the basis of activation of an integrated beta-galactosidase gene. J. Virol. 66, 2232–2239.
Kobe, B., Center, R.J., Kemp, B.E., Poumbourios, P., 1999. Crystal structure of human T cell leukemia virus type 1 gp21 ectodomain crystallized as a maltose-binding protein chimera reveals structural evolution of retroviral transmembrane proteins. Proc. Natl. Acad. Sci. U.S.A. 96, 4319–4324.
Kodama, E.I., Kohgo, S., Kitano, K., Machida, H., Gatanaga, H., Shigeta, S., Matsuoka, M., Ohrui, H., Mitsuya, H., 2001. 4′-Ethynyl nucleoside analogs: potent inhibitors of multidrug-resistant human immunodeficiency virus variants in vitro. Antimicrob. Agents Chemother. 45, 1539–1546.
Lalezari, J.P., Henry, K., O'Hearn, M., Montaner, J.S., Piliero, P.J., Trottier, B., Walmsley, S., Cohen, C., Kuritzkes, D.R., Eron Jr., J.J., Chung, J., DeMasi, R., Donatacci, L., Drobnes, C., Delehanty, J., Salgo, M., 2003. Enfuvirtide, an HIV-1 fusion inhibitor, for drug-resistant HIV infection in North and South America. N. Engl. J. Med. 348, 2175–2185.
Lazzarin, A., Clotet, B., Cooper, D., Reynes, J., Arasteh, K., Nelson, M., Katlama, C., Stellbrink, H.J., Delfraissy, J.F., Lange, J., Huson, L., DeMasi, R., Wat, C., Delehanty, J., Drobnes, C., Salgo, M., 2003. Efficacy of enfuvirtide in patients infected with drug-resistant HIV-1 in Europe and Australia. N. Engl. J. Med. 348, 2186–2195.
Liu, S., Jing, W., Cheung, B., Lu, H., Sun, J., Yan, X., Niu, J., Farmar, J., Wu, S., Jiang, S., 2007. HIV gp41 C-terminal heptad repeat contains multifunctional domains. Relation to mechanisms of action of anti-HIV peptides. J. Biol. Chem. 282, 9612–9620.
Liu, S., Lu, H., Niu, J., Xu, Y., Wu, S., Jiang, S., 2005. Different from the HIV fusion inhibitor C34, the anti-HIV drug Fuzeon (T-20) inhibits HIV-1 entry by targeting multiple sites in gp41 and gp120. J. Biol. Chem. 280, 11259–11273.
Medinas, R.J., Lambert, D.M., Tompkins, W.A., 2002. C-terminal gp40 peptide analogs inhibit feline immunodeficiency virus: cell fusion and virus spread. J. Virol. 76, 9079–9086.
Mink, M., Mosier, S.M., Janumpalli, S., Davison, D., Jin, L., Melby, T., Sista, P., Erickson, J., Lambert, D., Stanfield-Oakley, S.A., Salgo, M., Cammack, N., Matthews, T., Greenberg, M.L., 2005. Impact of human immunodeficiency virus type 1 gp41 amino acid substitutions selected during enfuvirtide treatment on gp41 binding and antiviral potency of enfuvirtide in vitro. J. Virol. 79, 12447–12454.
Nameki, D., Kodama, E., Ikeuchi, M., Mabuchi, N., Otaka, A., Tamamura, H., Ohno, M., Fujii, N., Matsuoka, M., 2005. Mutations conferring resistance to human immunodeficiency virus type 1 fusion inhibitors are restricted by gp41 and Rev-responsive element functions. J. Virol. 79, 764–770.
Otaka, A., Nakamura, M., Nameki, D., Kodama, E., Uchiyama, S., Nakamura, S., Nakano, H., Tamamura, H., Kobayashi, Y., Matsuoka, M., Fujii, N., 2002. Remodeling of gp41-C34 peptide leads to highly effective inhibitors of the fusion of HIV-1 with target cells. Angew. Chem. Int. Ed. Engl. 41, 2937–2940.
Poveda, E., Rodés, B., Toro, C., Martín-Carbonero, L., Gonzalez-Lahoz, J., Soriano, V., 2002. Evolution of the gp41 env region in HIV-infected patients receiving T-20, a fusion inhibitor. AIDS 16, 1959–1961.
Rimsky, L.T., Shugars, D.C., Matthews, T.J., 1998. Determinants of human immunodeficiency virus type 1 resistance to gp41-derived inhibitory peptides. J. Virol. 72, 986–993.
Root, M.J., Kay, M.S., Kim, P.S., 2001. Protein design of an HIV-1 entry inhibitor. Science 291, 884–888.
Ryu, J.R., Lee, J., Choo, S., Yoon, S.H., Woo, E.R., Yu, Y.G., 1998. Development of an in vitro assay system for screening of gp41 inhibitory compounds. Mol. Cells 8, 717–723.
Schibli, D.J., Weissenhorn, W., 2004. Class I and class II viral fusion protein structures reveal similar principles in membrane fusion. Mol. Membr. Biol. 21, 361–371.
Tagat, J.R., McCombie, S.W., Nazareno, D., Labroli, M.A., Xiao, Y., Steensma, R.W., Strizki, J.M., Baroudy, B.M., Cox, K., Lachowicz, J., Varty, G., Watkins, R., 2004. Piperazine-based CCR5 antagonists as HIV-1 inhibitors. IV. Discovery of 1-[(4,6-dimethyl-5-pyrimidinyl)carbonyl]-4-[4-[2-methoxy-1(*R*)-4-(trifluoromethyl)phenyl]ethyl-3(*S*)-methyl-1-piperazinyl]-4-methylpiperidine (Sch-417690/Sch-D), a potent, highly selective, and orally bioavailable CCR5 antagonist. J. Med. Chem. 47, 2405–2408.
Watanabe, S., Takada, A., Watanabe, T., Ito, H., Kida, H., Kawaoka, Y., 2000. Functional importance of the coiled-coil of the Ebola virus glycoprotein. J. Virol. 74, 10194–10201.
Wei, X., Decker, J.M., Liu, H., Zhang, Z., Arani, R.B., Kilby, J.M., Saag, M.S., Wu, X., Shaw, G.M., Kappes, J.C., 2002. Emergence of resistant human immunodeficiency virus type 1 in patients receiving fusion inhibitor (T-20) monotherapy. Antimicrob. Agents Chemother. 46, 1896–1905.
Wexler-Cohen, Y., Shai, Y., 2007. Demonstrating the C-terminal boundary of the HIV 1 fusion conformation in a dynamic ongoing fusion process and implication for fusion inhibition. FASEB J. 21, 3677–3684.
Xu, Y., Hixon, M.S., Dawson, P.E., Janda, K.D., 2007. Development of a FRET assay for monitoring of HIV gp41 core disruption. J. Org. Chem. 72, 6700–6707.

Bioorganic & Medicinal Chemistry Letters 18 (2008) 4124–4129

Contents lists available at ScienceDirect

Bioorganic & Medicinal Chemistry Letters

journal homepage: www.elsevier.com/locate/bmcl

Identification of novel non-peptide CXCR4 antagonists by ligand-based design approach

Satoshi Ueda [a], Manabu Kato [a], Shinsuke Inuki [a], Hiroaki Ohno [a], Barry Evans [b], Zi-xuan Wang [b], Stephen C. Peiper [b], Kazuki Izumi [c], Eiichi Kodama [c], Masao Matsuoka [c], Hideko Nagasawa [d], Shinya Oishi [a,*], Nobutaka Fujii [a,*]

[a] Graduate School of Pharmaceutical Sciences, Kyoto University, Sakyo-ku, Kyoto 606-8501, Japan
[b] Department of Pathology, Medical College of Georgia, GA 30912, USA
[c] Institute for Virus Research, Kyoto University, Sakyo-ku, Kyoto 606-8507, Japan
[d] Gifu Pharmaceutical University, Mitahora-higashi, Gifu 502-8585, Japan

ARTICLE INFO

Article history:
Received 6 April 2008
Revised 21 May 2008
Accepted 22 May 2008
Available online 29 May 2008

Keywords:
Chemokine
CXCR4
SDF-1
Anti-HIV
Indole

ABSTRACT

The design and synthesis of novel non-peptide CXCR4 antagonists is described. The peptide backbone of highly potent cyclic peptide-based CXCR4 antagonists was entirely replaced by an indole framework, which was expected to reproduce the disposition of the key pharmacophores consistent with those of potential bioactive conformations of the original peptides. A structure–activity relationship study on a series of modified indoles identified novel small-molecule antagonists having three pharmacophore functional groups through the appropriate linkers.

Chemokines are a family of small proteins with chemotactic and proactivatory effects on leukocytes. Chemokines mediate their biological effects by binding to the specific G-protein coupled receptor subtypes that are differentially and widely expressed in blood cells. Among these chemokine receptors, CXCR4 has a broad tissue distribution and the activation by its endogenous ligand CXCL12 (SDF-1, stromal cell-derived factor 1) leads to chemotaxis, immunomodulation, and other regulatory functions including progenitor cell migration during embryologic development of the cardiovascular, hematopoietic, and central nervous systems. In addition to its physiological roles, CXCR4 also plays important roles in pathological conditions. These include tumor growth and metastasis[1] and rheumatoid arthritis (RA).[2] CXCR4 has also been reported to act as a major co-receptor involved in the entry of T-cell-line-tropic human immunodeficiency virus type 1 (HIV-1) strains into target cells.[3] Thus, CXCR4 is considered as an important therapeutic target for multiple diseases. Inhibitory compounds of CXCL12 or HIV-1 binding to CXCR4 could be novel classes of anti-cancer, anti-RA, and anti-HIV-1 drugs. Previously, we found highly potent peptide-based CXCR4 antagonists such as **1**, **2**, and **3** (Fig. 1).[4,5]

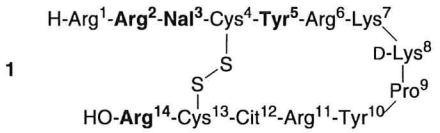

1

2 cyclo(-D-Tyr[1]-**L-Arg[2]-L-Arg[3]-L-Nal[4]**-L-Gly[5]-)

3 cyclo(-**D-Tyr[1]**-D-Arg[2]-**L-Arg[3]-L-Nal[4]**-L-Gly[5]-)

Figure 1. Structures of **1** and its downsized peptides **2** and **3**. Bold residues are the indispensable residues for the potent CXCR4-antagonistic activity. Nal, L-3-(2-naphthyl)alanine; Cit, L-citrulline.

Peptide **1** and its derivatives effectively blocked X4-HIV-1 entry to the cell by specifically binding to CXCR4,[6] and also showed an anti-metastatic effect against breast cancer[7] and anti-RA activity[8] in mouse models.

Although peptides are excellent lead molecules for development of pharmaceutical agents, special drug delivery systems are usually required for their clinical use because of the poor bioavailability and instability against enzymes. Whereas several peptide-based CXCR4 antagonists have been reported, only small numbers of small-molecule CXCR4 antagonists have been

* Corresponding authors. Tel: +81 75 753 4551; fax: +81 75 753 4570 (N. Fujii).
E-mail addresses: soishi@pharm.kyoto-u.ac.jp (S. Oishi), nfujii@pharm.kyoto-u.ac.jp (N. Fujii).

0960-894X/$ - see front matter © 2008 Elsevier Ltd. All rights reserved.
doi:10.1016/j.bmcl.2008.05.092

reported.[9] These prompted us to design novel non-peptide CXCR4 antagonists based on the SAR and conformational studies on peptide ligands **1**–**3**.

Cyclic pentapeptide-based CXCR4 antagonists **2** and **3** were identified by screening of cyclic pentapeptide libraries, which were designed based on SAR studies of peptide **1**. The constrained backbone of the cyclic peptide was utilized as a template for positioning the key functional groups in space as is found in parent peptide **1**. Subsequent conformational analysis of **2** permitted us to determine the topology of the four indispensable residues, then, rational approach toward the de novo design of non-peptide antagonists may be envisaged.[10]

Our previous SAR studies on **2** and its derivatives have shown that at least three functional groups on the peptide side-chains are required: (1) an aromatic ring such as 2-naphthyl- or 3-indolyl group at position 4; (2) a guanidino group at position 3; (3) a guanidino group at position 2 or a phenol group at position 1.[11] However, it was difficult to determine the spatial relationships between these functional groups due to the free rotation of the side-chain torsion (χ) angles. In our structural analyses, peptide **2** adopted a

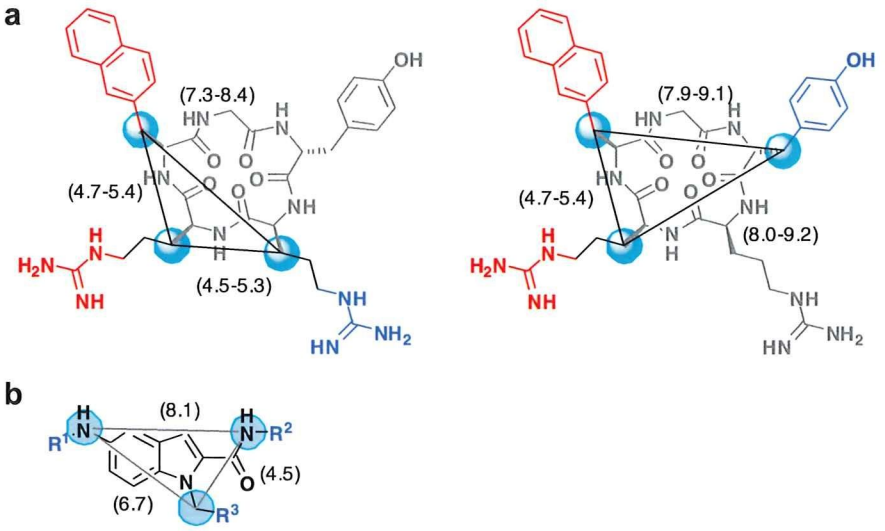

Figure 2. Design of indole-based CXCR4 antagonists based on molecular dynamics calculation of **2**. Distances (Å) between Cβ atoms bearing three essential functional groups during 1000 ps MD calculation of **2** (a) and between two key atoms of energy-minimized 5-acetamido-1-methylindole-2-carboxamide (b) are shown in parentheses. R^1–R^3 include naphthyl, indolyl, guanidino, and phenol groups.

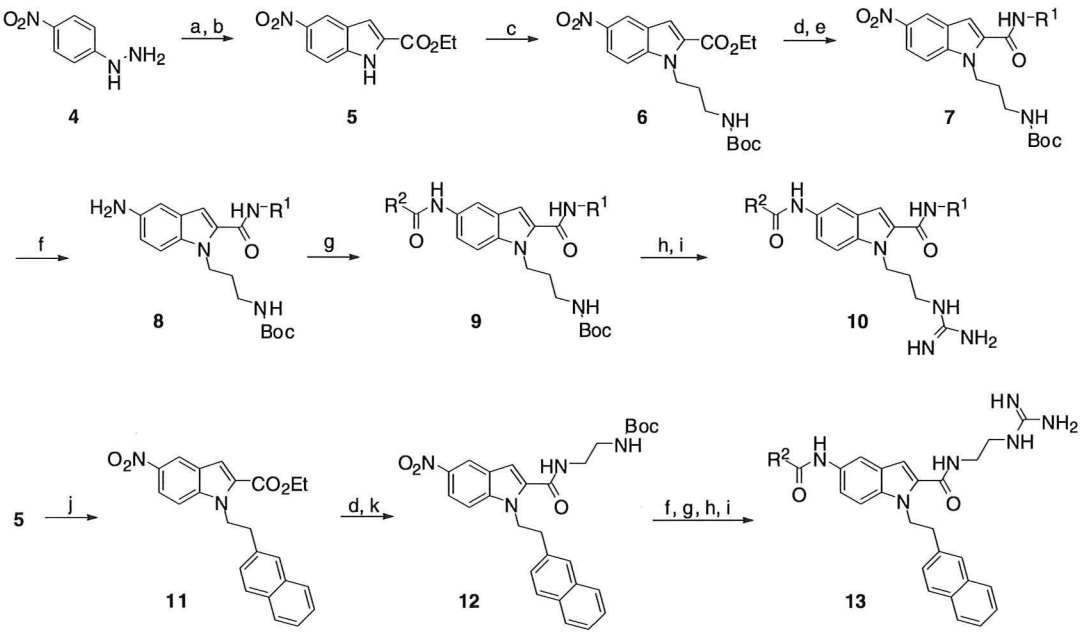

Scheme 1. Reagents and conditions; (a) ethyl pyruvate, EtOH, reflux; (b) polyphosphoric acid, xylene, 130°C; (c) NaH, *N*-Boc-3-bromopropylamine, DMF, 70 °C; (d) 1 N NaOH aq., EtOH-THF; (e) R^1-NH_2, HATU, Et_3N, DMF; (f) NH_4CO_2H, Pd/C, EtOH-THF, reflux; (g) R^2-CO_2H, HATU, Et_3N, DMF; (h) 95% TFA-H_2O; (i) 1-*H*-pyrazolecarboxamidine hydrochloride, Et_3N, DMF; (j) 2-(2-naphthyl)ethyl bromide, NaH, DMF, 70 °C; (k) *N*-Boc-ethylenediamine, HATU, Et_3N, DMF.

variety of global conformations, in which the distances between indispensable functional groups were variable. On the other hand, relatively rigid cyclic peptide backbone and fixed distances between Cβ atoms, which append key functional groups, were observed.[5] Hence, we envisioned that introduction of crucial functional moieties for receptor binding onto a bicyclic heterocycle scaffold, which mimics the relatively fixed cyclic pentapeptide backbone of **2**, would provide non-peptide CXCR4 ligands. In this letter, we report a part of our ongoing research to develop novel non-peptide small molecule CXCR4 antagonists.

Among several molecular scaffold candidates, we first selected 5-aminoindole-2-carboxylic acid for the following reasons: (1) molecular modeling suggested that it met the spatial requirements for displaying the three key substituents (Fig. 2);[12] (2) accessible synthetic approaches were available for attachment of the three substituents; (3) indoles represent an important class of bioactive compounds and the physicochemical properties in terms of medicinal chemistry are well-documented.

Syntheses of indole-based compounds were achieved as shown in Scheme 1. (4-Nitrophenyl)hydrazine **4** was converted to the corresponding hydrazone, which was subjected to Fischer ring closure reaction to produce an indole **5**. Alkylation of N^1 position of the indole **5** with *N*-Boc-3-bromopropylamine gave **6**. This was hydrolyzed using 1 N aqueous sodium

Table 1
Inhibitory activities of indole derivatives **10a–j** and **13a–b** against binding of ^{125}I-SDF-1α to CXCR4

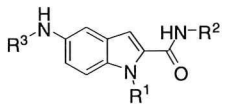

Compound	R^1	R^2	R^3	% inhibition at 10 μM
10a	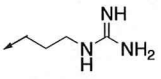	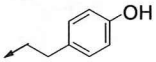	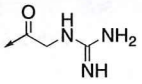	23
10b	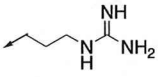	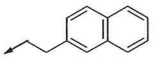	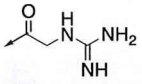	63
10c	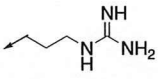	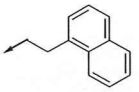	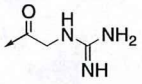	61
10d	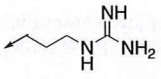	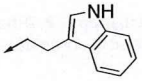	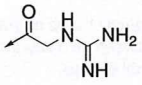	88
10e	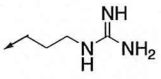	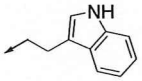	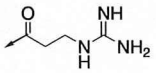	70
10f	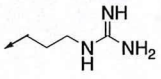	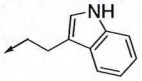	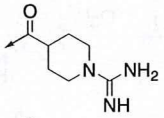	86
10g[a]	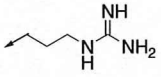	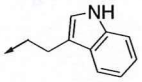	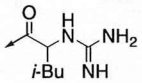	77
10h[a]	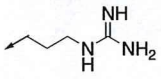	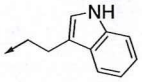	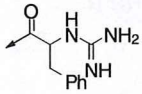	72
10i	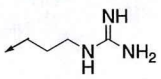		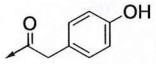	62
10j	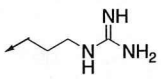		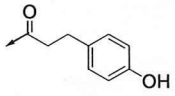	55
13a	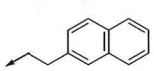	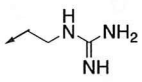	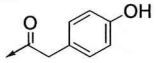	51
13b	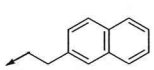	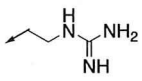	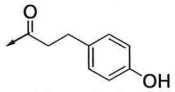	53

[a] Evaluated as a racemic mixture.

hydroxide in EtOH-THF and the resulting free carboxylic acid was coupled with amines using *O*-(7-azabenzotriazol-1-yl)-1,1,3,3-tetramethyluronium hexafluorophosphate (HATU) as coupling reagent to give **7**. The nitro group of **7** was reduced to amine **8** upon treatment with Pd-C and ammonium formate in EtOH. The aminoindole **8** was then coupled with carboxylic acids to give **9**. Deprotection of Boc group(s) by 95% TFA and guanylation of the free amino group(s) produced the target compounds **10**. Another series of compounds **13** were synthesized from **5** using similar reaction sequences described for **10**.

All indole-based compounds listed in Tables 1 and 2 were purified by preparative reverse-phase HPLC (purity >95%) and characterized by MALDI-TOF-MS. These compounds were tested for competitive binding inhibition in human CXCR4 transfected Chinese hamster ovary (CHO) cells using [^{125}I]SDF-1 as a radioligand, with the results given as percentage inhibition at 10 μM. IC_{50} values of selected compounds are shown in Table 2.

Compound **10d** with 2-(3-indolyl)ethyl group at the R^2 position showed 88% inhibition at 10 μM (IC_{50} = 3.0 μM) and was more potent than compounds having (4-hydroxyphenyl)-, (1-naphthyl)- or (2-naphthyl)-alkyl group at the R^2 position (compounds **10a–c**, 23–63% inhibition at 10 μM). Further SAR studies based on **10d** were undertaken. Chain elongation of the guanidinoacetyl group (R^3) of **10d** caused slight decrease in the affinity (**10e**). The use of *N*-amidinopiperidine-4-carbonyl was also acceptable for high potency [IC_{50} (**10f**) = 3.0 μM]. Introduction of an isobutyl or benzyl group into the α-carbon of guanidinomethyl carbonyl group of **10d** did not cause significant drop in binding affinity (compounds **10g** and **10h**). Compounds with *S*-configuration at the chiral center showed more potent CXCR4 antagonistic activity as compared with the corresponding *R*-isomers. (***S***)-**10g** was identified as the most potent compound [IC_{50} ((***S***)-**10g**) = 1.2 μM].[13] Compound (***S***)-**10g** also showed potent anti-HIV-1 activity (IIIB strain, inhibition of HIV-1 induced cytopathogenicity: EC_{50} = 5.4 μM). The IC_{50} value of (***S***)-**10g** is 34-fold lower as compared with parent peptide **2**. This is probably due to the absence of phenol functionality in (***S***)-**10g** which corresponds to D-Tyr side-chain of peptide **2**. Decreased number of amide bond in (***S***)-**10g** might also lead to the lower affinity. We have previously showed the importance of backbone amide functionalities of **2** for CXCR4 antagonistic activity by using reduced-amide isosteres or (*E*)-alkene dipeptide isosteres.[14]

Indole-based compounds having a phenol group at R^3 position showed moderate CXCR4-binding affinity (**10i**, **10j**, **13a**, and **13b**). Interestingly, these compounds did not show complete inhibition even at higher concentrations in the binding inhibition experiments, while compounds having a guanidino group at R^3 position (**10c**, **10d**, and (***S***)-**10g**) achieved complete inhibition (Fig. 3). These results suggest that **10c**, **10d** and (***S***)-**10g** are inhibitors that competitively bind to the SDF-1 binding site of CXCR4, while **10i**, **10j**, **13a**, and **13b** may bind to an allosteric site of CXCR4 and partially antagonize the SDF-1 binding.

Comparison of energy-minimized structures of (***S***)-**10g** and previously reported solution conformation of **2** revealed that three functional groups on the indole template well overlapped the three pharmacophore residues of **2** as expected. In this model, indole scaffold favorably mimicked the backbone of Arg–Arg–Nal sequence of **2** (see Fig. 4).

In summary, a series of indole-based compounds were designed, synthesized, and characterized as a novel class of CXCR4 antagonists. Although their IC_{50} values are in the μM range, these indole derivatives could serve as a useful lead for further medicinal chemistry programs.

Table 2
IC_{50} values of selected indole derivatives

Compound	Structure	IC_{50} (μM)
10d	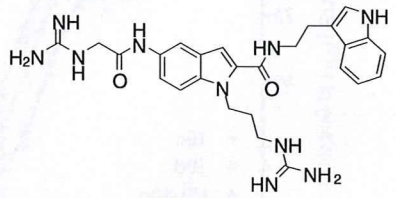	3.0
10f	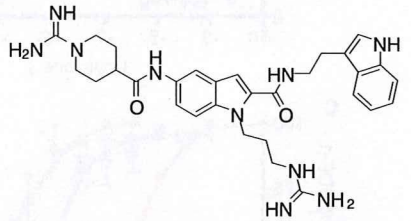	3.0
(***S***)-**10g**	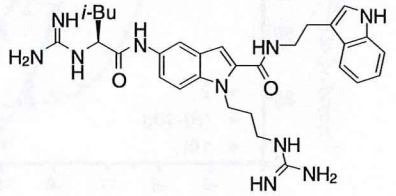	1.2
(***R***)-**10g**	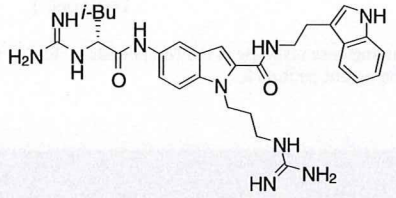	2.2
(***S***)-**10h**	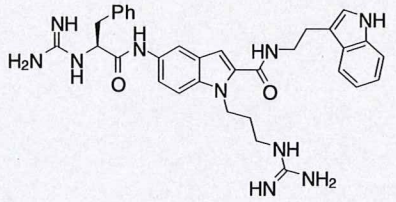	1.7
(***R***)-**10h**	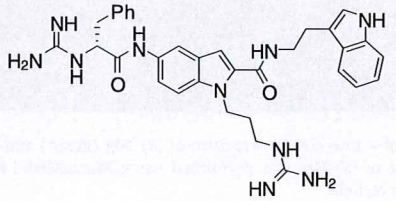	3.7
10i	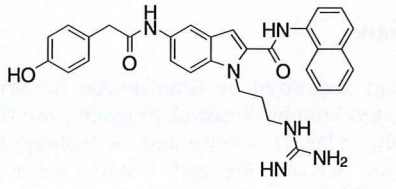	4.8
13b	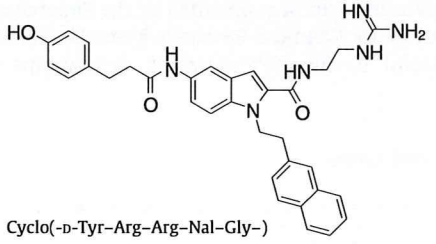	2.7
2	Cyclo(-D-Tyr–Arg–Arg–Nal–Gly–)	0.035

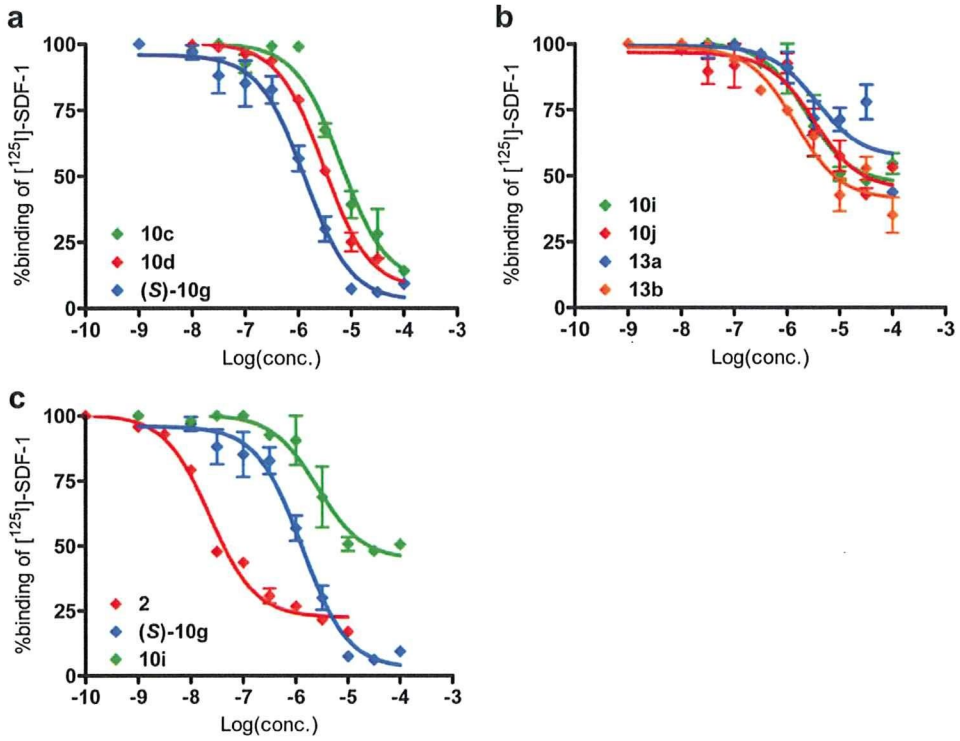

Figure 3. Ligand binding dose response of the compounds (a) having two guanidino pharmacophores and (b) having a phenol pharmacophore, and (c) the comparison of the two subsets with the parent peptide **2**.

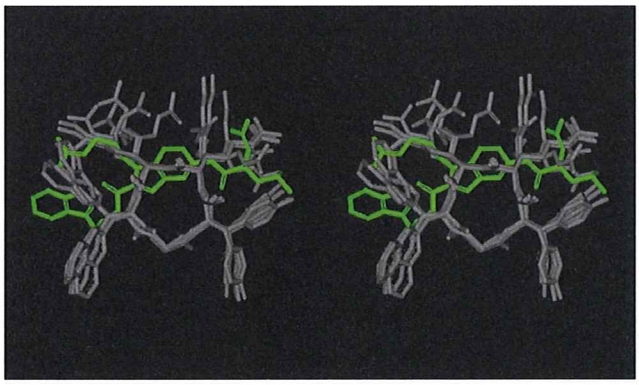

Figure 4. Overlay of a low-energy structure of (***S***)-**10g** (green) and **2** (gray). The molecular modeling of (***S***)-**10g** was performed using MacroModel-Program (Ver. 8.1) with 'MMFF' force field.

Acknowledgments

This work was supported by Grant-in-Aid for Scientific Research and Targeted Proteins Research Program from the Ministry of Education, Culture, Sports, Science, and Technology of Japan, and Health and Labour Sciences Research Grants (Research on HIV/AIDS). Computation time was provided by the Supercomputer Laboratory, Institute for Chemical Research, Kyoto University. S.U. and S.I. are grateful to the JSPS Research Fellowships for Young Scientists.

References and notes

1. Müller, A.; Homey, B.; Soto, H.; Ge, N.; Catron, D.; Buchanan, M. E.; Mcclanahan, T.; Murphy, E.; Yuan, W.; Wagner, S. M.; Barrera, J. L.; Mohar, A.; Verástegui, E.; Zlotnik, A. *Nature* **2001**, *410*, 50.
2. Nanki, T.; Hayashida, K.; El-Gabalawy, H. S.; Suson, S.; Shi, K.; Girschick, H. J.; Yavuz, S.; Lipsky, P. E. *J. Immunol.* **2000**, *165*, 6590.
3. Oberlin, E.; Amara, A.; Bachelerie, F.; Bessia, C.; Virelizier, J. L.; Arenzana-Seisdedos, F.; Schwartz, O.; Heard, J. M.; Clark-Lewis, I.; Legler, D. L.; Loetscher, M.; Baggiolini, M.; Moser, B. *Nature* **1996**, *382*, 833.
4. Masuda, M.; Nakashima, H.; Ueda, T.; Naba, H.; Ikoma, R.; Otaka, A.; Terakawa, Y.; Tamamura, H.; Ibuka, T.; Murakami, T.; Koyanagi, Y.; Waki, M.; Matsumoto, A.; Yamamoto, N.; Funakoshi, S.; Fujii, N. *Biochem. Biophys. Res. Commun.* **1992**, *189*, 845.
5. Fujii, N.; Oishi, S.; Hiramatsu, K.; Araki, T.; Ueda, S.; Tamamura, H.; Otaka, A.; Kusano, S.; Terakubo, S.; Nakashima, H.; Broach, J. A.; Trent, J. O.; Wang, Z.; Peiper, S. C. *Angew. Chem. Int. Ed.* **2003**, *42*, 3251.
6. Tamamura, H.; Xu, Y.; Hattori, T.; Zhang, X.; Arakaki, R.; Kanbara, K.; Omagari, A.; Otaka, A.; Ibuka, T.; Yamamoto, N.; Nakashima, H.; Fujii, N. *Biochem. Biophys. Res. Commun.* **1998**, *253*, 877.
7. (a) Tamamura, H.; Hori, A.; Kanzaki, N.; Hiramatsu, K.; Mizumoto, M.; Nakashima, H.; Yamamoto, N.; Otaka, A.; Fujii, N. *FEBS Lett.* **2003**, *550*, 79; (b) Takenaga, M.; Tamamura, H.; Hiramatsu, K.; Nakamura, N.; Yamaguchi, Y.; Kitagawa, A.; Kawai, S.; Nakashima, H.; Fujii, N.; Igarashi, R. *Biochem. Biophys. Res. Commun.* **2004**, *320*, 226.
8. Tamamura, H.; Fujisawa, M.; Hiramatsu, K.; Mizumoto, M.; Nakashima, H.; Yamamoto, N.; Otaka, A.; Fujii, N. *FEBS Lett.* **2004**, *569*, 99.
9. (a) Donzella, G. A.; Schols, D.; Lin, S. W.; Este, J. A.; Nagashima, K. A.; Maddon, P. J. *Nat. Med.* **1998**, *4*, 72; (b) Ichiya, K.; Yokoyama-Kumakura, S.; Tanaka, Y.; Tanaka, R.; Hirose, K.; Bannai, K.; Edamatsu, T.; Yanaka, M.; Niitani, Y.; Miyano-Kurosaki, N.; Takaku, H.; Koyanagi, Y.; Yamamoto, N. *Proc. Natl. Acad. Sci. U.S.A.* **2003**, *100*, 4185; (c) Tamamura, H.; Ojida, A.; Ogawa, T.; Tsutsumi, H.; Masuno, H.; Nakashima, H.; Yamamoto, N.; Hamachi, I.; Fujii, N. *J. Med. Chem.* **2006**, *49*, 3412; (d) Zhan, W.; Liang, Z.; Zhu, A.; Kurtkaya, S.; Shim, H.; Snyder, J. P.; Liotta, D. C. *J. Med. Chem.* **2007**, *50*, 5655.
10. Conversion of peptide to nonpeptide by scaffolding strategy, see: (a) Hirschmann, R.; Nicolaou, K. C.; Pietranico, S.; Salvino, J.; Leahy, E. M.; Sprengeler, P. A.; Furst, G.; Strader, C. D.; Cascieri, M. A.; Candelore, M. R.; Donaldson; Cindy; Vale, W.; Maechler, L. *J. Am. Chem. Soc.* **1992**, *114*, 9217; (b) Kawato, H. C.; Nakayama, K.; Inagaki, H.; Ohta, T. *Org. Lett.* **2001**, *3*, 3451; (c) Nakayama, K.; Kawato, H. C.; Inagaki, H.; Ohta, T. *Org. Lett.* **2001**, *3*, 3447.
11. (a) Ueda, S.; Oishi, S.; Wang, Z.-x.; Araki, T.; Tamamura, H.; Cluzeau, J.; Ohno, H.; Kusano, S.; Nakashima, H.; Trent, J. O.; Peiper, S. C.; Fujii, N. *J. Med. Chem.* **2007**, *50*, 192; (b) Tamamura, H.; Araki, T.; Ueda, S.; Wang, Z.; Oishi, S.; Esaka, A.; Trent, J. O.; Nakashima, H.; Yamamoto, N.; Peiper, S. C.; Otaka, A.; Fujii, N. *J. Med. Chem.* **2005**, *48*, 3280.
12. Distances (Å) between β-carbons of **2** during 1000 ps MD calculation; D-Tyr^1–Arg^3: 8.0–9.2, D-Tyr^1–Nal^4: 7.9–9.1, Arg^3–Nal^4: 4.7–5.4, Arg^2–Arg^3: 4.5–5.3, Arg^2–Nal^4: 7.3–8.4, Arg^3–Nal^4: 4.7–5.4. Distances (Å) between two key atoms of energy-minimized 5-acetamido-1-methylindole-2-carboxamide:

(acetamide N)-(*N*-methyl C), 6.7; (acetamide N)-(carboxamide N), 8.1; (methyl C)-(carboxamide N), 4.5.

13. Compound (***S***)-**10g**: $[\alpha]_D^{23}$ − 6.4(*c*0.35, CH_3OH); ^1H NMR (500 MHz, DMSO-d_6): δ = 0.93 (d, *J* = 6.0 Hz, 3H), 0.95 (d, *J* = 5.9 Hz, 3H), 1.60–1.76 (m, 3H), 1.92 (tt, *J* = 6.6, 7.2 Hz, 2H), 2.97 (t, *J* = 7.6 Hz, 2H), 3.14 (dt, *J* = 6.2, 6.6 Hz, 2H), 3.55 (dt, *J* = 6.7, 7.0 Hz, 2H), 4.26–4.41 (m, 1H), 4.55 (t, *J* = 7.2 Hz, 2H), 6.86–7.53 (brm, 8H), 6.99 (m, 1H), 7.03–7.11 (m, 2H), 7.20 (br, 1H), 7.33–7.43 (m, 2H), 7.55 (d, *J* = 9.0 Hz, 1H), 7.59 (d, *J* = 7.9 Hz, 1H), 7.73 (t, *J* = 5.4 Hz, 1H), 7.90 (d, *J* = 9.0 Hz, 1H), 7.95–7.99, (br, 1H), 8.65 (t, *J* = 5.7 Hz, 1H), 10.08 (s, 1H), 10.82 (s, 1H); LRMS (FAB): 573 (MH^+, base peak), 444; HRMS (FAB): calcd for $C_{30}H_{41}N_{10}O_2$ (MH^+) 573.3414; found 573.3418. Compound (***S***)-**10h**: $[\alpha]_D^{23}$ 3.3(*c*0.34, CH_3OH); ^1H NMR (500 MHz, DMSO-d_6): δ = 1.91 (tt, *J* = 7.2, 7.4 Hz, 2H), 2.96 (t, *J* = 7.3 Hz, 2H), 2.97–3.04 (m, 1H), 3.13 (dt, *J* = 5.4, 7.2 Hz, 2H), 3.20–3.27 (m, 1H), 3.54 (dt, *J* = 6.0, 7.3 Hz, 2H), 4.54 (t, *J* = 7.4 Hz, 2H), 4.56–4.62 (m, 1H), 6.78–7.64 (brm, 8H), 6.98 (m, 1H), 7.03–7.10 (m, 2H), 7.19 (m, 1H), 7.21–7.27 (m, 1H), 7.27-7.40 (m, 6H), 7.55 (d, *J* = 8.9 Hz, 1H), 7.58 (d, *J* = 7.7 Hz, 1H), 7.71 (t, *J* = 5.3 Hz, 1H), 7.85 (d, *J* = 8.9 Hz, 1H), 7.89–7.92, (br, 1H), 8.64 (t, *J* = 6.0 Hz, 1H), 10.12 (br, 1H), 10.82 (br, 1H); LRMS (FAB): 607 (MH^+, base peak), 444; HRMS (FAB): calcd for $C_{33}H_{39}N_{10}O_2$ (MH^+) 607.3257; found 607.3251.
14. Tamamura, H.; Hiramatsu, K.; Ueda, S.; Wang, Z.; Kusano, S.; Terakubo, S.; Trent, J. O.; Peiper, S. C.; Yamamoto, N.; Nakashima, H.; Otaka, A.; Fujii, N. *J. Med. Chem.* **2005**, *48*, 380.

The International Journal of Biochemistry & Cell Biology 40 (2008) 2410–2420

Contents lists available at ScienceDirect

The International Journal of Biochemistry & Cell Biology

journal homepage: www.elsevier.com/locate/biocel

2′-Deoxy-4′-*C*-ethynyl-2-halo-adenosines active against drug-resistant human immunodeficiency virus type 1 variants

Atsushi Kawamoto[a], Eiichi Kodama[a,*], Stefan G. Sarafianos[b], Yasuko Sakagami[a], Satoru Kohgo[c], Kenji Kitano[c], Noriyuki Ashida[c], Yuko Iwai[c], Hiroyuki Hayakawa[c], Hirotomo Nakata[d,e], Hiroaki Mitsuya[d,e], Eddy Arnold[f], Masao Matsuoka[a]

[a] *Laboratory of Virus Immunology, Institute for Virus Research, Kyoto University, 53 Kawaramachi, Shogoin, Sakyo-ku, Kyoto 606-8507, Japan*
[b] *Department of Molecular Microbiology and Immunology, University of Missouri-Columbia, School of Medicine and Christopher S. Bond Life Sciences Center, Columbia, MO 65211, USA*
[c] *Biochemicals Division, Yamasa Corporation, Chiba 288-0056, Japan*
[d] *Department of Hematology and Infectious Diseases, Kumamoto University School of Medicine, Kumamoto 860-8556, Japan*
[e] *Experimental Retrovirology Section, HIV and AIDS Malignancy Branch, National Cancer Institute, Bethesda, MD 20892, USA*
[f] *Center for Advanced Biotechnology and Medicine and Department of Chemistry and Chemical Biology, Rutgers University, Piscataway, NJ 08854, USA*

ARTICLE INFO

Article history:
Received 3 December 2007
Received in revised form 14 March 2008
Accepted 2 April 2008
Available online 11 April 2008

Keywords:
Human immunodeficiency virus
Reverse transcriptase inhibitor
Resistance

ABSTRACT

One of the formidable challenges in therapy of infections by human immunodeficiency virus (HIV) is the emergence of drug-resistant variants that attenuate the efficacy of highly active antiretroviral therapy (HAART). We have recently introduced 4′-ethynyl-nucleoside analogs as nucleoside reverse transcriptase inhibitors (NRTIs) that could be developed as therapeutics for treatment of HIV infections. In this study, we present 2′-deoxy-4′-*C*-ethynyl-2-fluoroadenosine (EFdA), a second generation 4′-ethynyl inhibitor that exerted highly potent activity against wild-type HIV-1 (EC_{50} ~ 0.07 nM). EFdA retains potency toward many HIV-1 resistant strains, including the multi-drug resistant clone HIV-$1_{A62V/V75I/F77L/F116Y/Q151M}$. The selectivity index of EFdA (cytotoxicity/inhibitory activity) is more favorable than all approved NRTIs used in HIV therapy. Furthermore, EFdA efficiently inhibited clinical isolates from patients heavily treated with multiple anti-HIV-1 drugs. EFdA appears to be primarily phosphorylated by the cellular 2′-deoxycytidine kinase (dCK) because: (a) the antiviral activity of EFdA was reduced by the addition of dC, which competes nucleosides phosphorylated by the dCK pathway, (b) the antiviral activity of EFdA was significantly reduced in dCK-deficient HT-1080/Ara-C^r cells, but restored after dCK transduction. Further, unlike other dA analogs, EFdA is completely resistant to degradation by adenosine deaminase. Moderate decrease in susceptibility to EFdA is conferred by a combination of three RT mutations (I142V, T165R, and M184V) that result in a significant decrease of viral fitness. Molecular modeling analysis suggests that the M184V/I substitutions may reduce anti-HIV activity of EFdA through steric hindrance between its 4′-ethynyl moiety and the V/I184 β-branched side chains. The present data suggest that EFdA, is a promising candidate for developing as a therapeutic agent for the treatment of individuals harboring multi-drug resistant HIV variants.

1. Introduction

Highly active antiretroviral therapies (HAART), combining two or more reverse transcriptase inhibitors (RTIs) and/or protease inhibitors, have been successful in sig-

* Corresponding author. Tel.: +81 75 751 3986; fax: +81 75 751 3986.
E-mail address: ekodama@virus.kyoto-u.ac.jp (E. Kodama).

1357-2725/$ – see front matter © 2008 Elsevier Ltd. All rights reserved.
doi:10.1016/j.biocel.2008.04.007

nificantly reducing viral loads and bringing about clinical benefits to the treatment of patients infected with human immunodeficiency virus type 1 (HIV-1). Although HAART improves prognosis for HIV-1 infected patients (Palella et al., 1998), drug-resistant viruses emerge during prolonged therapy and some resistant viruses show intra-class cross resistance. Moreover, drug-resistant variants can be transmitted to other individuals as primary infections (Little et al., 2002). Hence, there is a great need for the development of new HIV inhibitors that retain activity against drug-resistant HIV variants.

In this regard, we have focused on the family of nucleoside reverse transcriptase inhibitors (NRTIs) and have previously reported that a series of 2′-deoxy-4′-*C*-ethynyl-nucleosides (EdNs) efficiently suppress (EC_{50}s as low as one nanomolar) various NRTI-resistant HIV strains including multi-drug resistant clinical isolates (Kodama et al., 2001). More recently, Haraguchi and others have reported that additional members of EdNs such as 2′,3′-didehydro-3′-deoxy-4′-*C*-ethynyl-thymidine (Ed4T) are also active against wild-type and drug-resistant strains (EC_{50}s ranged from 0.16 to 17 μM) and less toxic than d4T (also known as stavudine) *in vitro* (Dutschman et al., 2004; Haraguchi et al., 2003), while 4′-Ed4T is only moderately active against (−)-2′,3′-dideoxy-3′-thiacytidine (3TC or lamivudine)-resistant HIV-1_{M184V} (Nitanda et al., 2005).

To further increase the antiviral activity and reduce the cytotoxicity, we designed and synthesized a second generation of 4′-substituted adenosine analogs with halogen substitutions at their 2-position. We report here that 2′-deoxy-4′-*C*-ethynyl-2-fluoroadenosine (EFdA) exhibits the highest antiviral activity than any other NRTI when assayed against wild-type or NRTI-resistant HIV clones and clinical isolates from patients treated extensively with anti-HIV agents. In addition, unlike other adenosine-based NRTIs, EFdA showed adenosine deaminase (ADA) resistance. We also show that EFdA is primarily activated through phosphorylation by cellular deoxycytidine kinase (dCK). Molecular modeling analysis has been used to rationalize the resistance profile of these analogs toward key NRTI mutations.

2. Materials and methods

2.1. Compounds

3′-Azido-3′-deoxythymidine (AZT, or zidovudine), 2′,3′-dideoxyinosine (ddI, or didanosine), and 2′,3′-dideoxycytidine (ddC, or zalcitabine) were purchased from Sigma (St. Louis, MO.). 3TC was kindly provided from S. Shigeta (Fukushima Medical University, Fukushima, Japan). A set of EdN analogs were designed and synthesized as described elsewhere (Ohrui, 2006). Their chemical structures are shown in Fig. 1. 2′-Deoxycoformycin (dCF) was synthesized in Yamasa Corporation (Choshi, Japan).

2.2. Cells and plasmids

MT-2 and MT-4 cells were grown in an RPMI 1640-based culture medium, and 293T cells were grown in Dulbecco's modified Eagle medium (DMEM); each of these media was

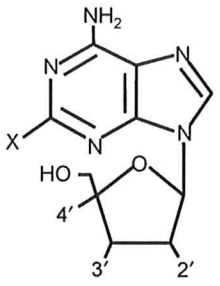

Base X	Sugar 2′	Sugar 3′	4′	Compound abbreviation
-H	-H	-OH	-C ≡ CH	*E*dA
-F	-H	-OH	-C ≡ CH	2F-*E*dA
-F	-H	-H	-C ≡ CH	2F-*E*ddA
-F	C = C		-C ≡ CH	2F-*E*d4A
-F	-H	-OH	-C ≡ N	2F-CNdA
-Cl	-H	-OH	-C ≡ CH	2Cl-*E*dA

Fig. 1. Structures of 4′-substituted adenosine analogs. All nucleoside analogs discussed here have substitutions at the 4′-position of the sugar ring.

supplemented with 10% fetal calf serum (FCS), 2 mM L-glutamine, 100 U/ml penicillin, and 50 μg/ml streptomycin. HeLa-CD4-LTR/β-galactosidase (MAGI) cells were propagated in DMEM supplemented with 10% FCS, 0.2 mg/ml of hygromycin B, and 0.2 mg/ml of G418 (Kimpton and Emerman, 1992). HeLa-CD4/CCR5-LTR/β-galactosidase cells were propagated in puromycin (10 μg/ml) containing DMEM with hygromycin and G418. Peripheral blood mononuclear cells (PBMCs) were obtained from healthy HIV-1-seronegative donors by Ficoll-Hypaque gradient centrifugation and stimulated for 3 days with phytohemagglutinin M (PHA; 10 μg/ml; Sigma) and recombinant human interleukin 2 (IL-2; 10 U/ml; Shionogi & Co., Ltd., Osaka, Japan) prior to use. Human fibrosarcoma cell lines, HT-1080 and HT-1080/Ara-C^r were grown in the RPMI-based culture medium (Obata et al., 2001). To express HIV-1 receptors, we constructed a mammalian expression vector pBC-CD4/CXCR4-IH, which encodes CD4, CXCR4, and hygromycin phosphotransferase with two internal ribosome entry sites under control of cytomegalovirus promoter as described (Kajiwara et al., 2006). After the transfection into HT-1080 and HT-1080/Ara-C^r, cells were selected by 0.2 mg/ml hygromycin B. For the expression of human deoxycytidine kinase (dCK), pCI-neo (Promega, Madison, WI)-based plasmid, pCI-dCK, was transfected into HT-1080/Ara-C^r and selected with 0.2 mg/ml G418. Established cells were designated HT-1080/Ara-C^r/dCK. Puromycin resistance gene under the control of PGK promoter was inserted into pLTR-SEAP (Miyake et al., 2003), which encodes a secreted form of the placental alkaline phosphatase (SEAP) gene under control of the HIV-1 long terminal repeat (LTR) (pLTR-SEAP-puro^r). pLTR-SEAP-puro^r was transfected into the three HT-1080 cell lines and selected with 10 μg/ml puromycin.

2.3. Viruses and construction of recombinant HIV-1 clones

Two laboratory strains, HIV-1_{IIIB} and HIV-2_{EHO}, were used. Multi-drug resistant clinical HIV-1 strains, which had been exposed to over 10 anti-HIV-1 drugs for at least 3 years, were passaged in PHA-stimulated PBMCs (PHA-PBMCs) and stored at −80 °C until further use. Recombinant infectious HIV-1 clones carrying various mutations in the *pol* gene were generated using pNL101 (Jeang et al., 1993). Briefly, desired mutations were introduced into the XmaI–NheI region (759 bp) of pTZNX1, which encoded Gly-15 to Ala-267 of HIV-1 RT (strain BH 10) by a site-directed mutagenesis method (Weiner et al., 1994). The XmaI–NheI fragment was inserted into a pNL101-based plasmid, pNL-RT, generating various molecular clones with the desired mutations. To generate pNL-RT, we first introduced a silent mutation at NheI site of the pNL101, GCTAGC to GCCAGC (underlined; 7251 n.t. from the 5′-LTR) by site-directed mutagenesis. Then, the ApaI–SalI fragment of pNL101 without the NheI site was replaced with that of pSUM9 (Shirasaka et al., 1995), to introduce XmaI and NheI site in the RT coding region. The presence of intended substitutions and the absence of unintended substitutions in the molecular clones were confirmed by sequencing. Each molecular clone (2 μg/ml as DNA) was transfected into 293T cells (4×10^5 cells/6-well plate) by FuGENE 6 Transfection Reagent (Roche Diagnostics, Indianapolis, IN). After 24 h, MT-2 cells (10^6 cells/well) were added and co-cultured with 293T cells for an additional 24 h. When an extensive cytopathic effect was observed, the cell supernatants were harvested, and the virus was further propagated in MT-4 cells. The culture supernatant was harvested and stored at −80 °C until further use.

2.4. Determination of drug susceptibility

The inhibitory effect of test compounds on viral replication for 5 days was evaluated in MT-4 cells by the MTT method as described previously (Kodama et al., 2001). The sensitivity of NRTI-resistant infectious clones to test compounds was determined by the MAGI assay as described (Nameki et al., 2005). The drug susceptibility of HIV-1 clinical isolates was determined on day 7 by a commercially available p24 antigen assay (Kodama et al., 2001). Briefly, PHA-PBMCs (10^6 cells/ml) were exposed to each viral preparation at $TCID_{50}$ of 50 and cultivated in 200 μl of culture medium containing various concentration of the drug in 96-well culture plates. All assays were performed in triplicate, and the amounts of p24 antigen produced by the cells into the culture medium were determined. A 2′-deoxynucleoside competition assay was performed by the same way as the MAGI assay. An adenosine deaminase (ADA) inhibitor, dCF, was added for preventing conversion of 2′-deoxyadenosine (dA) to 2′-deoxyinosine (dI) (final concentration 0.4 μM). The effect of dCK expression on activities of test compounds was examined by measurement of SEAP activity in the supernatant. At first, the target cells (HT-1080, HT-1080/Ara-C^r, and HT-1080/Ara-C^r/dCK) were suspended in 96-well plates (5.0×10^3 cells/well). On the following day, the cells were inoculated with HIV-1_{IIIB} (500 MAGI unit/well, giving 500 blue cells in MAGI cells) in the presence of serially diluted compounds. After 48 h incubation, supernatant was collected and SEAP activity in the supernatant was measured using BD Great EscAPe SEAP chemiluminescence detection kit (BD Biosciences Clontech., Palo Alto, CA) and Wallac 1450 MicroBeta Jet Luminometer (PerkinElmer, Wellesley, MA).

2.5. The effect of ADA

The effect of ADA on EdA or EFdA was examined by high performance liquid chromatography (HPLC). ADA (0.01 U) derived from bovine intestinal tract was added into 0.5 ml of 0.5 mM EFdA in 50 mM Tris–HCl buffer (pH 7.5), and incubated at 25 °C. Samples were collected each 15 min and analyzed by HPLC.

2.6. HIV-1 replication assays

MT-2 cells (2.5×10^5 cells/5 ml) were infected with each virus preparation (500 MAGI units) for 4 h. The infected cells were then washed and cultured in a final volume of 5 ml. Culture supernatants (200 μl) were harvested from days 1 to 7 after infection, and the p24 antigen amounts were quantified (Nameki et al., 2005).

For competitive HIV-1 replication assay (CHRA), two titrated infectious clones to be examined were mixed and added to MT-2 cells (10^5 cells/3 ml) as described previously (Kosalaraksa et al., 1999; Nameki et al., 2005). To ensure that the two infectious clones being compared were of approximately equal infectivity, a fixed amount (500 MAGI units) of one infectious clone was mixed with three different amounts (250, 500 and 1000 MAGI units) of the other infectious clone. On day 1, one-third of the infected MT-2 cells were harvested, washed twice with phosphate-buffered saline, and the cellular DNA was extracted. The purified DNA was subjected to nested PCR and then direct DNA sequencing. The HIV-1 coculture which best approximated a 50:50 mixture on day 1 was further propagated. Every 4–6 days, the cell-free supernatant of the virus coculture (1 ml) was transmitted to new uninfected MT-2 cells. The cells harvested at the end of each passage were subjected to direct sequencing, and the viral population change was determined by the relative peak height in the sequencing chromatogram. The persistence of the original amino acid substitution was confirmed in all infectious clones used in this assay.

2.7. Molecular modeling studies

The programs SYBYL and O were used to prepare models of the complexes of wild-type, M184V, and insertion mutant HIV-1 RT with DNA and the triphosphates of 3TC and EFdA. The starting atomic coordinates of HIV-1 RT were from the structure described by Huang et al. (PDB code 1RTD) (Huang et al., 1998). The side-chain mutations were manually modeled using mostly conformations encountered in RT structures that carry such mutations. The local structures of mutants were optimized using energy minimization protocols in SYBYL. The triphosphates of the inhibitors were built based on the structures of dTTP in

Table 1
Antiviral activity against HIV-1 and HIV-2 strains in MT-4 cells

Compound (abbreviation)	EC_{50} (μM)[a]		Selectivity[b]	
	HIV-1_{IIIB}	HIV-2_{EHO}	CC_{50} (μM)[c]	index
2′-Deoxy-4′-C-ethynyl-adenosine (EdA)	0.0095 ± 0.0027[d]	0.006 ± 0.0015	104 ± 6.2	11,000
2′-Deoxy-4′-C-ethynyl-2-fluoroadenosine (EFdA)	0.000073 ± 0.000017	0.000098 ± 0.000022	9.8 ± 3.4	134,000
2′,3′-Dideoxy-4′-C-ethynyl-2-fluoroadenosine (EFddA)	1.17 ± 0.29	1.07 ± 0.23	230 ± 33	196
2′,3′-Didehydro-3′-deoxy-4′-C-ethynyl-2-fluoroadenosine (EFd4A)	0.11 ± 0.033	0.089 ± 0.0007	98 ± 26	899
2′-Deoxy-4′-C-cyano-2-fluoroadenosine (CNFdA)	0.1 ± 0.034	0.09 ± 0.0087	>340	>3,300
2′-Deoxy-4′-C-ethynyl-2-chloroadenosine (ECldA)	0.00069 ± 0.00018	0.0006 ± 0.0000028	230 ± 16	339,000
2′,3′-Dideoxyinosine (ddI)	27 ± 12	24 ± 4.4	>100	>4
3′-Azido-3′-deoxythymidine (AZT)	0.0028 ± 0.00062	0.0022 ± 0.00073	30 ± 7.2	10,800

Anti-HIV activity was determined by the MTT method.
[a] EC_{50} represents the concentration that blocks HIV-1 replication by 50%.
[b] Selectivity index is calculated by the CC_{50}/EC_{50} for HIV-1_{IIIB}.
[c] CC_{50} represents the concentration that suppress the viability of HIV-1-unexposed cells by 50%.
[d] Data shown are mean values with standard deviations for at least three independent experiments.

1RTD, or of tenofovir diphosphate in the ternary complex of HIV-1 RT/DNA/TFV-DP (Tuske et al., 2004).

3. Results

3.1. Antiviral activity of 4′- and 2-substituted deoxyadenosine analogs

We evaluated the activity of 4′- and 2-substituted deoxyadenosine analogs against HIV-1 with the MTT assay using MT-4 cells. The 2′-deoxy-4′-*C*-ethynyl nucleoside with adenine as the base (EdA) exerted comparable activity to AZT (Table 1). 2-Fluoro substituted EdA, EFdA, was the most potent against HIV-1 with a sub-nanomolar EC_{50} of 0.073 nM. Selectivity of EFdA and ECldA was much increased compared to parental EdA or AZT. However, EFdA was also relatively cytotoxic compared to other inhibitors of this series. The 2-chloro (Cl) substitution also provided enhanced activity but with a decreased toxicity. Further modifications of the sugar ring from 2′-deoxyribose to 2′,3′-dideoxy- or 2′, 3′-didehydro-2′,3′-dideoxy-ribose (EFddA or EFd4A) resulted in a drastic decrease of inhibitory potential. Substitution of the 4′-E group with a structurally similar 4′-cyano group also resulted in markedly decreased inhibitory activity. These results indicate that the 3′-OH and 4′-E moieties in the sugar ring are indispensable for high efficacy, and that antiviral activities are augmented by the modification with F- or Cl-moiety at the adenine 2-position. These compounds suppressed the replication of HIV-2 at comparable levels as HIV-1, consistent with the hypothesis that they act as nucleoside reverse transcriptase inhibitors (De Clercq, 1998).

3.2. Antiviral activity against HIV-1 variants resistant to NRTIs

To assess the effect of 4′- and 2-substituted adenosine analogs against drug resistant HIV-1, we generated recombinant infectious clones carrying various NRTI resistant mutations and tested them using the MAGI assay. We found that EdA, EFdA, and ECldA efficiently suppressed many of the viruses resistant to approved NRTI including the multi-drug resistant (MDR) virus, although the 3TC-resistant variant HIV-1_{M184V} and the multi-drug resistant variant HIV-$1_{M41L/T69SSG/T215Y}$ (Winters et al., 1998) showed modestly increased EC_{50} values to these compounds (Table 2). Interestingly, highly active 4′-E analogs, which have 3′-OH such as EFdA or ECldA, were even more effective against the dideoxy-type NRTI resistant variants K65R, L74V, and Q151M complex than they were against WT RT (Table 2). In contrast, 4′-E analogs without 3′-OH (EFddA and EFd4A) were similar or less effective with these resistant variants compared to WT, although the effect seems to be minimal. EFd4A and 2′-deoxy-4′-*C*-cyano-2-fluoroadenosine (CNFdA) were moderately active against HIV-1_{WT} and HIV-1_{MDR} (Shirasaka et al., 1995), but less active against HIV-1_{M184V}. Susceptibility of even the least active EFddA was still in the low micromolar range, but decreased against both HIV-1_{M184V} and HIV-1_{MDR}, by 84- and 13-fold, respectively.

3.3. Antiviral activity of EFdA against multi-drug resistant clinical isolates

We went on to further characterize EFdA, the most potent compound of the series, against clinical isolates from patients exposed to many anti-AIDS drugs. Five multi-drug resistant strains (HIV-1_{IVR405}, HIV-1_{IVR406}, HIV-1_{IVR412}, HIV-1_{IVR413}, and HIV-1_{A03}), which contained various drug-resistance mutations in HIV-1 genes (Table 3), were used. These clinical isolates showed high resistance to AZT, 3TC (HIV-1_{IVR406}), and ddI (HIV-1_{IVR412}). HIV-1_{IVR415} was also a drug-experienced virus but did not have NRTI-resistance mutations and showed no resistance, or less resistance to the NRTIs tested. Hence, it was used as a drug-sensitive HIV-1. Although antiviral activity of EFdA was slightly reduced against HIV-$1_{IVR405, IVR406, IVR412}$ (5.7- to 7.6-fold) compared to HIV-1_{IVR415}, the activity was high enough to suppress viral replication. It should be emphasized that EFdA was active against HIV-1_{IVR406}, which had the 3TC-resistant M184I substitution.

To evaluate antiviral activity of EFdA to M184V containing isolates in detail, two isolates harboring M184V were used. We used the MAGI assay that directly determines inhibition on a single replication cycle of HIV-1, so that we could eliminate the possible effects of multiple repli-

Table 2
Anti HIV-1 activity against drug-resistant infectious clones

	EC_{50} (μM)[a]								
	EdA	EFdA	EFddA	EFd4A	CNFdA	EClda	ddI	AZT	3TC
WT	0.021	0.0011	1.2	0.35	0.21	0.0064	4.1	0.015	0.71
K65R	0.0082	0.00023 (×0.2)	1.56	0.2	ND[b]	0.0017 (×0.3)	ND	0.0039 (×0.3)	ND
L74V	0.01	0.00048 (×0.4)	2.52	0.54	ND	0.0015 (×0.2)	14.6	0.019 (×1.3)	ND
V75T	0.0075	0.00067 (×0.6)	9.13	0.95	ND	0.005 (×0.8)	ND	0.047 (×3.1)	ND
M41L/T215Y	0.062	0.0016 (×1.5)	6.7	1.67	ND	0.0065 (×0.1)	ND	0.12 (×8)	ND
M41L/T69SSG/T215Y[c]	0.18	0.0065 (×6)	ND	ND	ND	0.025 (×4)	21	0.20 (×13)	9.9
MDR[d]	0.011	0.00074 (×0.7)	16	0.46	0.69	0.0057 (×0.9)	40	18 (×1200)	1.1
P119S	0.018	0.00067 (×0.6)	ND	ND	ND	0.0062 (×1)	ND	0.0033 (×0.2)	0.6
T165A	0.045	0.001 (×0.9)	ND	ND	ND	0.0082 (×1.3)	ND	ND	0.66
I142V	0.077	0.001 (×0.9)	ND	ND	ND	0.0062 (×1)	ND	0.016 (×1)	0.36
T165R	0.088	0.0016 (×1.5)	ND	ND	ND	0.012 (×1.9)	ND	0.011 (×0.7)	0.28
M184V	0.088	0.0083 (×7.5)	101	6.41	1.76	0.084 (×13)	ND	0.0021 (×0.1)	>100
T165R/M184V	0.6	0.014 (×13)	ND	ND	ND	0.17 (×27)	ND	0.0053 (×0.4)	>100
I142V/T165R/M184V	0.81	0.023 (×22)	ND	ND	ND	0.41 (×65)	ND	0.0076 (×0.5)	>100
T165A/M184V[e]	0.43	0.015 (×14)	ND	ND	ND	0.16 (×25)	ND	0.0049 (×0.3)	>100
P119S/T165A/M184V[e]	0.5	0.015 (×14)	ND	ND	ND	0.20 (×32)	ND	0.0043 (×0.3)	>100

Anti-HIV activity was determined with the MAGI assay.

[a] The data shown are mean values obtained from the results of at least three independent experiments.

[b] ND: not determined.

[c] HIV-1 variant contains T69S substitution and 6-base pair insertions between codons for 69 and 70 (Ser-Gly) with AZT resistant mutations M41L/T215Y (Winters et al., 1998).

[d] Multi-dideoxynucleoside resistant HIV-1 contains mutations (AGT-GGT, SG) in the *pol* region: A62V/V75I/F77L/F116Y/Q151M (Shirasaka et al., 1995).

[e] These variants were reported by Nitanda et al. during induction of Ed4T resistant variants.

cation cycles on measured antiviral activity. In this assay, EFdA effectively suppressed both replication of HIV-1_{IVR443} and HIV-1_{IVR463}. Compared to the EC_{50} value for HIV-1_{WT} in Table 2, reduction of the activity was less than 3-fold, suggesting that EFdA suppresses relatively efficiently 3TC-resistant variants with either M184I or M184V mutations.

3.4. ADA stability of EFdA

Cellular ADA is known to convert dA to dI through deamination. Phosphorylation of the deaminated dA analogs, *e.g.*, dI, is less efficient, resulting in low conversion of the active triphosphate (TP) form. In order to assess if the activation of these compounds to their TP forms would be affected by the activity of ADA, we tested whether ADA can degrade EdA or EFdA. While EdA was almost completely deaminated after 90 min exposure to ADA, EFdA was not deaminated for up to at least 90 min (Fig. 2). These results indicate that the 2-halo-substitution in EdA confers significant resistance to degradation by ADA.

3.5. Phosphorylation of EFdA

Currently available NRTIs need to be converted to the TP form by host cellular kinases before incorporation into newly synthesized proviral DNA. It has been shown that the antiviral effect of NRTIs was reversed by the addition of their physiological counterpart 2′-deoxynucleosides (Bhalla et al., 1990; Mitsuya et al., 1985). To identify the phosphorylation pathway, we examined whether the antiviral activity of EFdA was reversed by the addition of 2′-deoxynucleosides. Surprisingly, the addition of dC decreased the antiviral activity of EFdA in a dose-dependent manner (Fig. 3). In contrast, dT and dG had no effect on the

Table 3
Antiviral activity of EFdA against clinical isolates

Clinical isolates	Amino acid substitutions in the reverse transcriptation	EC_{50} (μM)			
		AZT	ddI	3TC	EFdA
PBMCs[a]					
IVR405	M41L/E44D/D67G/V118I/Q151M/L210W/T215Y	1.76	2.45	0.55	0.0012
IVR406	M41L/E44D/D67N/V118I/M184I/L210W/T215Y/K219R	0.64	1.46	>10	0.0011
IVR412	M41L/E44D/V75L/A98S/L210W/T215F	3.97	9.11	0.83	0.0016
IVR413	M41L/E44D/D67N/V75L/A98S/V118I/L210W/T215Y/K219R	1.0	2.22	1.46	0.00021
A03	M41L/E44D/D67N/L74V/L100I/K103N/V118I/L210W/T215Y	0.53	2.15	0.49	0.0001
IVR415	None	0.0028	0.33	0.078	0.00021
MAGI cells[b]					
IVR443	I135T/Y181C/M184V	0.027	3.6	>100	0.0031
IVR463	M41L/E44D/D67N/M184V/H208Y/L210W/T215Y	0.31	7.5	>100	0.0032

All assays were performed in triplicate. AZT, ddI, and 3TC were served as a control.

[a] Antiviral activity was determined by the inhibition of p24 antigen production in the culture supernatant.

[b] HeLa-CD4/CCR5-LTR/β-gal cells was used for the MAGI assay.